

HELSINKI INSTITUTE OF PHYSICS

INTERNAL REPORT SERIES

HIP-1999-03

QUANTUM SIMULATIONS OF ATOM-PHOTON INTERACTIONS

MARTTI HAVUKAINEN

Helsinki Institute of Physics
University of Helsinki
Helsinki, Finland

Academic dissertation

*To be presented, with the permission of the Faculty of Science
of the University of Helsinki, for public criticism in Auditorium XII
on October 9th, 1999, at 10 o'clock a.m.*

Helsinki 1999

ISBN 951-45-8709-X (PDF version)
Helsingin yliopiston verkkojulkaisut
Helsinki 1999

Preface

This work has been done at Helsinki Institute of Physics (HIP). I am most grateful to Prof. Stig Stenholm for his guidance and giving me possibility to do this work. I am also greatly indebted to Doc. K.-A. Suominen. Part of the work was done in his group. I also thank Prof. V. Bužek and G. Drobný for collaboration and for their hospitality during my visit in Bratislava.

I want to thank my parents and little sister about everything. I also thank the members of the group of Quantum Optics who have helped me in numerous problems. Finally I thank all my friends especially in our bowling and minigolf group. They have helped me during my studies and together we have had many tight matches.

I also want to thank the Center for Scientific Computing (CSC) for offering their computer facilities for this work.

With gratitude I acknowledge the financial support provided by the Academy of Finland.

Helsinki, September 1999

Martti Havukainen

Contents

Preface	i
Abstract	iv
List of publications	v
Contribution by the author	vi
1 Introduction	1
2 Canonical quantization of the field	3
2.1 A free field	3
2.2 An interacting field	5
3 Methods to solve the problem of interacting systems	7
3.1 Master equations	7
3.2 Cascaded master equations	8
3.3 The excitation expansion	10
3.4 The correlation function expansion	11
4 The stochastic harmonic oscillator	12
5 The spectrum of the radiation field	16
5.1 Mode spectrum	16
5.2 Fourier spectrum	16
5.3 Generalizations of Fourier spectrum	17
5.4 Physical spectrum	18
5.5 Analyser atom spectrum	19
6 Cavity QED simulations in 1D	21
7 Cavity QED simulations in 2D	28
7.1 The general theory	28
7.2 Various simulations	30
7.2.1 A free photon	30
7.2.2 A mirror	31
7.2.3 A beam splitter	32
7.2.4 A parabolic mirror	33

7.2.5	A mirror box	34
7.2.6	Circular cavities	34
7.2.7	Decay of an atom in a square cavity	37
7.3	Possible future simulations	39
8	Conclusion	40
	Appendix: Numerics	41
A.1	Different languages used in the simulations	41
A.1.1	Fortran	41
A.1.2	C and C++	42
A.1.3	Java	42
	References	44

Abstract

There have been several different definitions for a time dependent spectrum. They are all based on various integrals over two time averages of certain operators. In paper I we show a new method to determine the spectrum of a radiation field. The method is closely related to a realistic spectrum measurement. The radiation we want to analyze is directed into a kind of spectrum detector which consists of two-level atoms. The radiation interacts with the detector and the spectrum can be read from the quantum mechanical state of the detector. The two time averages used normally in the determination of the spectrum are not needed. In paper I the method is applied to the resonance fluorescence radiation of a laser-driven three-level atom and the spectrum obtained is compared to the one calculated with traditional definitions. In paper V we show that the same method can be used to detect the local mode spectrum.

In paper II we study the time evolution of a trapped electron inside an electromagnetic trap. We use a phenomenological model for the dynamics. The electron moves in a harmonic potential. The depth of the potential depends on the spin direction, which changes stochastically. The ensemble density matrix is seen to approach a thermal-like state.

In papers III and VI we present the results of simulations in a one-dimensional cavity. Inside the cavity there are many two-level atoms. We have studied the atomic decay near the mirrors and inside a crystal built of two-level atoms. In paper IV we extend the one-dimensional simulations of papers III, V and VI to two dimensions. We show that using two level atoms it is possible to build mirrors and beam splitters for the radiation. Several layers of atoms which are exactly on resonance with the radiation form a mirror. One layer of off-resonant atoms is a beam splitter. It is possible to build complicated optical networks using quantum mechanical mirrors and beam splitters. Using mirrors it is possible to build closed cavities of arbitrary shape. It is also possible to use moving atoms which allows moving mirrors and beam splitters to be built.

List of publications

This thesis consists of an introductory review part, followed by six research publications:

- I *An open-systems approach to calculating time-dependent spectra*
M. Havukainen and S. Stenholm
Journal of Modern Optics **45**(8), 1699-1716 (1998)

- II *Coherence properties of the stochastic oscillator*
M. Havukainen and S. Stenholm
Physical Review A **60**, 621-629 (1999)

- III *Numerical simulations of fundamental processes in cavity QED: Atomic decay*
V. Bužek, G. Drobný, M. G. Kim, M. Havukainen and P. L. Knight
Physical Review A **60**, 582-592 (1999)

- IV *Quantum simulations of optical systems*
M. Havukainen, G. Drobný, S. Stenholm and V. Bužek
Journal of Modern Optics **46**(9), 1343-1367 (1999)

- V *Comparisons of spectra determined using detector atoms and spatial correlation functions*
M. Havukainen
LANL: quant-ph/9909019
HIP: HIP-1999-50/TH

- VI *Stimulated emission via quantum interference: Scattering of one-photon packets on an atom in a ground state*
G. Drobný, M. Havukainen and V. Bužek
LANL:
HIP: HIP-1999-55/TH

The internet version of the thesis can be found on the web page
<http://www.hip.fi/~quantum/theses/havukainen/>.

Author's contribution

My contribution to all papers has been essential. In paper I, I developed the method to use two-level atoms and cascaded master equations to determine the time dependent spectrum. I did all the computer simulations and wrote most of the text. I did all the simulations for paper II and wrote part of the paper. For paper III I did part of the simulations. I generalized the methods introduced in paper III to two dimensions and developed some important numerical techniques. I invented the idea to use the atoms to model optical components, did all the simulations and wrote most of the text. Paper V contains only my contribution. I did the computer simulations and wrote the text. I did part of the computer simulations for paper VI.

1 Introduction

It is an experimental fact that white light can be divided into light of different colors with prisms. Mathematically white light is composed of light with several different wave lengths. It has turned out to be difficult to give a good mathematical definition of a spectrum. Almost all quantum mechanical definitions are Fourier transforms over two time correlation functions. The natural spectrum is, of course, time dependent. The usual method to include time dependence into the theoretical definitions has been to restrict the correlations taken into account. It can be argued that this is because every realistic spectrum detector has a filling time which restricts the accuracy of the measurement. However, it is not obvious why spectrum detectors should detect something which is related to two time averages. In papers I and V we develop a model for a spectrum detector. The radiation we want to analyze is directed onto a group of two-level atoms. The atoms have very small line widths. Only radiation which is exactly on resonance can excite them. The excitation probability is proportional to the intensity. When the excitation is measured with atoms with different resonance frequencies, we can interpret the excitation as a function of frequency and time as a time dependent spectrum. In paper I the method is used to determine the time dependent spectrum of a laser-driven three-level atom. The method is shown to give the same spectrum as the one calculated using two time averages. In paper V we use the method in one-dimensional cavity QED simulations and compare the results to the local mode spectrum obtained by filtered spatial correlation functions.

Mirrors and beam splitters are usually treated as classical objects which interact with light. They are modelled by a 2×2 matrix which operates on the two input ports and directs the modified beams to the outputs. Usually the canonical quantization of the field is done in free space with periodic boundary conditions. It is possible to do this in the presence of mirrors. The first thing to do is to determine the modes of the system. The mirrors are included by using appropriate boundary conditions. It is possible to do the same with beam splitters using more complicated boundary conditions. After the modes have been calculated, the coefficients in the field expansion should be interpreted as operators instead of complex numbers as in the quantization of a free field. However, this approach is difficult, especially if the mirror and beam splitter configuration is complicated. Even more difficult is to quantize the system if the mirrors and beam splitters are moving. In that case the mode functions are time dependent.

We have been able to treat mirrors and beam splitters in some special cases. We consider many two-level atoms inside a two-dimensional cavity. The state vector of the

system is restricted to have only a single excitation. The interaction between the field and the atoms is of the Jaynes-Cummings form, which guarantees that the state vector preserves its single excitation form. In paper IV we show that it is possible to build beam splitters and mirrors using two-level atoms with appropriate parameters. Several layers of atoms form a mirror if the distance between the atoms is small enough, the dipole coupling with the field is strong enough and the atoms are on resonance with the incoming radiation. Similarly one layer of off-resonant atoms forms a beam splitter. Both components may have an arbitrary shape. We have used plane, parabolic and closed circular mirrors.

Special numerical techniques to integrate the time evolution have been developed. A very important point is that it is possible to utilize the Fast Fourier Transform (FFT) in the integration. This makes some simulations orders of magnitudes faster. Because of FFT it is possible to include thousands, maybe tens of thousands, of atoms in the simulations. This allows us to build complicated mirror and beam splitter configurations used in real experiments. It is also possible to use moving atoms.

In these simulations, the whole system is in a quantum mechanical state. The difficult calculation of the mode functions, which would be needed if the mirrors and beam splitters would be treated classically, is not needed. The main limitation of the simulations is that the field strength is restricted to one photon only.

It is possible to trap a single electron using magnetic field and laser light. It can be shown that the electron experiences a harmonic potential inside the trap. The depth of the potential is determined by the direction of the spin of the electron. The direction of the spin changes stochastically. In paper II we study the time evolution of an electron inside a trap. The initial state in the simulations is a pure state. The ensemble state of the electron is seen to lose coherence at greater time values.

In paper III we study the decay of a two-level atom inside a dielectric material. The dielectric material is modelled using different configurations of two-level atoms. The general result is that the decay is slower than the free space decay. In paper VI we study the scattering of the photon on an atom in one dimension. The photon has various different initial states. The state of the field is seen to have a significant effect on the atomic excitation.

2 Canonical quantization of the field

2.1 A free field

In the 19th century J. C. Maxwell was able to explain several phenomena related to electric charges and electric and magnetic fields. He introduced the equations [1]

$$\nabla \times \mathbf{E}(\mathbf{r}, t) = -\frac{\partial}{\partial t} \mathbf{B}(\mathbf{r}, t), \quad (1)$$

$$\nabla \times \mathbf{B}(\mathbf{r}, t) = \frac{1}{c^2} \frac{\partial}{\partial t} \mathbf{E}(\mathbf{r}, t), \quad (2)$$

$$\nabla \cdot \mathbf{E}(\mathbf{r}, t) = \frac{\rho}{\epsilon_0}, \quad (3)$$

$$\nabla \cdot \mathbf{B}(\mathbf{r}, t) = 0. \quad (4)$$

These equations determine the time evolution of electric \mathbf{E} and magnetic \mathbf{B} fields if boundary conditions including the charge distribution ρ are known. The same equations can be used to describe also quantum fields if the electric and magnetic vectors are interpreted as operators. The quantization of the field was first done by P. A. M. Dirac in 1927 [2, 3].

In the quantization process in free space ($\rho = 0$), the field is imagined to be enclosed inside a box of length L . The values of the coordinates are restricted to $-\frac{L}{2} \leq x, y, z \leq \frac{L}{2}$. The usual choice is to use periodic boundary conditions (PBC) and plane wave basis functions $e^{i\mathbf{k}\cdot\mathbf{r}}$. Naturally the boundary conditions are not physical but they can be used if the nonzero field is concentrated near the origin. The \mathbf{E} and \mathbf{B} fields can be expanded using the basis functions as [4, 5, 6, 7]

$$\hat{\mathbf{E}}(\mathbf{r}, t) = \frac{1}{L^{3/2}} \sum_{\mathbf{k}_s} \left(\frac{\hbar}{2\omega_{\mathbf{k}_s}\epsilon_0} \right)^{1/2} \left[\hat{a}_{\mathbf{k}_s}(0) \epsilon_{\mathbf{k}_s} e^{i(\mathbf{k}\cdot\mathbf{r}-\omega t)} + \text{h.c.} \right] \quad (5)$$

$$\hat{\mathbf{B}}(\mathbf{r}, t) = \frac{1}{L^{3/2}} \sum_{\mathbf{k}_s} \left(\frac{\hbar\omega_{\mathbf{k}_s}}{2\epsilon_0} \right)^{1/2} \left[i\hat{a}_{\mathbf{k}_s}(0) \epsilon_{\mathbf{k}_s} e^{i(\mathbf{k}\cdot\mathbf{r}-\omega t)} + \text{h.c.} \right]. \quad (6)$$

The crucial point in the quantization process is to interpret the dimensionless coefficients of the basis functions as creation $\hat{a}_{\mathbf{k}_s}^\dagger$ and annihilation $\hat{a}_{\mathbf{k}_s}$ operators introduced in the quantization of a harmonic oscillator. The operators obey the commutation relations

$$\begin{aligned}
[\hat{a}_{\mathbf{k}s}, \hat{a}_{\mathbf{k}'s'}^\dagger] &= \delta_{\mathbf{k}\mathbf{k}'}\delta_{ss'}, \\
[\hat{a}_{\mathbf{k}s}, \hat{a}_{\mathbf{k}'s'}] &= [\hat{a}_{\mathbf{k}s}^\dagger, \hat{a}_{\mathbf{k}'s'}^\dagger] = 0.
\end{aligned} \tag{7}$$

For the electric and magnetic field operators at a specific time we get, using equations (5)-(7), the commutation relations

$$[\hat{E}_i(\mathbf{r}_1, t), \hat{E}_j(\mathbf{r}_2, t)] = 0, \tag{8}$$

$$[\hat{B}_i(\mathbf{r}_1, t), \hat{B}_j(\mathbf{r}_2, t)] = 0, \tag{9}$$

$$[\hat{E}_i(\mathbf{r}_1, t), \hat{B}_j(\mathbf{r}_2, t)] = \frac{\hbar}{i\epsilon_0} \sum_{l=1}^3 \epsilon_{ijl} \frac{\partial}{\partial r_{1l}} \delta^3(\mathbf{r}_1 - \mathbf{r}_2). \tag{10}$$

The Hamiltonian for the free field is the integral of the energy density over the quantization volume

$$\hat{H} = \int_L d^3r \left[\frac{1}{2} \epsilon_0 \hat{\mathbf{E}}^2(\mathbf{r}, t) + \frac{1}{2\mu_0} \hat{\mathbf{B}}^2(\mathbf{r}, t) \right] \tag{11}$$

$$= \sum_{\mathbf{k}s} \hbar\omega_{\mathbf{k}s} (\hat{a}_{\mathbf{k}s}^\dagger \hat{a}_{\mathbf{k}s} + \frac{1}{2}), \tag{12}$$

where the orthogonality of the basis functions is used. The formulation where the time evolution of the system is included in the operators is called the Heisenberg picture and is formally quite similar to the classical equations. In the Heisenberg picture the equation of motion for operators is

$$i\hbar \frac{\partial \hat{A}}{\partial t} = [\hat{A}, \hat{H}], \tag{13}$$

where the Hamiltonian is given by the equation (11). For electric and magnetic fields using the commutators (8)-(10) we get exactly Maxwell's equations (1) and (2).

For a quantum mechanical system, all knowledge of a particle can be described by the quantum mechanical state vector $|\Psi\rangle$. The time evolution of a state is given by the Schrödinger equation

$$i\hbar \frac{\partial |\Psi\rangle}{\partial t} = \hat{H}|\Psi\rangle. \tag{14}$$

The same approach can be used for the field. The field is expanded using basis states which are tensor products of single mode Fock-states

$$|\{n\}\rangle = \prod_{\mathbf{k}} |n_{\mathbf{k}}\rangle. \quad (15)$$

The general state of the field can be written as

$$|\Psi\rangle = \sum_{\{n\}} c_{\{n\}} |\{n\}\rangle \quad (16)$$

where $c_{\{n\}}$ are coefficients of the basis vectors. The equation of motion for the field is the same as in the single particle case (14), and the Hamiltonian is given by equation (11).

The equations of motion for a field are easy to write down but for a realistic fields almost impossible to solve directly. The difficulty is that the basis states with nonzero coefficients are enormously numerous, and in computer simulations demand a lot of memory. The weakness of the periodic mode functions $e^{i\mathbf{k}\cdot\mathbf{r}}$ is that they are delocalized over the whole cavity. Almost all realistic fields are more localized so a basis with a localized spatial energy density distribution and a finite width of its frequency distribution would be better.

2.2 An interacting field

So far we have considered the field in free space. Next we add an atomic Hamiltonian \hat{H}_A and an interaction between the atoms and the field. The detailed form of \hat{H}_A depends on the nature of the atomic part. There are several alternatives for deriving the interaction between the matter and the field. One approach is to use the minimal substitution. The momentum of the atomic Hamiltonian is replaced by the kinetic momentum

$$\hat{\mathbf{p}} \rightarrow \hat{\mathbf{p}} - e\hat{\mathbf{A}}(\mathbf{r}, t), \quad (17)$$

where $\hat{\mathbf{A}}(\mathbf{r}, t)$ is the vector potential of the field and $-e$ is the charge of the electron. This gives, if the field is weak enough, the interaction Hamiltonian within the dipole approximation [4, 5]

$$\hat{H}_I(t) = -\frac{e}{m}\hat{\mathbf{p}}(t) \cdot \hat{\mathbf{A}}(\mathbf{r}_0, t). \quad (18)$$

The vector potential is evaluated at the position of the atom. The approximation can be done if the width of the wave function is smaller than the wave length of the

radiation. It is convenient to apply the unitary transform $U = \exp(-i\mathbf{e}\mathbf{r} \cdot \mathbf{A}(\mathbf{r}_0, t)/\hbar)$ to the Hamiltonian $\hat{H}_F + \hat{H}_A$. As a result we get for the interaction term

$$\hat{H}_I = -\frac{e}{\epsilon_0} \mathbf{r} \cdot \hat{\mathbf{D}}(\mathbf{r}_0, t). \quad (19)$$

The dielectric displacement vector operator $\hat{\mathbf{D}}(\mathbf{r}, t)$ can in most cases be replaced by the electric field operator $\hat{\mathbf{E}} = \frac{1}{\epsilon_0} \hat{\mathbf{D}}$.

Using the expansion (5) for the electric field and the creation and annihilation operator form for the position operator we get, after the rotating wave approximation (RWA), for the interaction Hamiltonian with the two-level atom

$$\hat{H}_I = g(|2\rangle\langle 1|\hat{a} + |1\rangle\langle 2|\hat{a}^\dagger), \quad (20)$$

where g is the coupling constant. In the RWA the terms $|2\rangle\langle 1|\hat{a}^\dagger$ and $|1\rangle\langle 2|\hat{a}$ are neglected. The coupling constant for these terms oscillates very rapidly and for time scales of interest will have a zero average. In summary, the total Hamiltonian for the system with atoms can be divided into three parts

$$\hat{H} = \hat{H}_F + \hat{H}_A + \hat{H}_I, \quad (21)$$

where \hat{H}_F is the field, \hat{H}_A the atomic and \hat{H}_I the interaction Hamiltonian.

3 Methods to solve the problem of interacting systems

The situation described by the Hamiltonian (21) is very typical in quantum optics and there are several approaches to determine the time evolution of the system. One of the traditional approaches is to trace out the field part of the Hilbert space and get an equation of motion, a master equation, for the atomic part of the system. There are several possibilities to take the field part into account in the simulations. We have used excitation expansion where the basis vectors of the field are restricted to have only a few excitations. Another method would be to use correlation functions to describe the state of the field.

3.1 Master equations

In the derivation of a master equation, two major approximations must be introduced. First, the interaction between the atomic and field parts must be weak so that the terms higher than second order in \hat{H}_I can be neglected. This is the Born approximation. The second, Markov approximation, demands that the future time evolution of the atomic part depends only on its present state and not on its state in the past. With these approximations the master equation takes the form

$$i\hbar \frac{\partial \hat{\rho}_A}{\partial t} = [\hat{H}_A, \hat{\rho}_A] + L[\hat{\rho}_A], \quad (22)$$

where $\hat{\rho}_A$ is the density matrix for the atomic part of the system. The first term on the right gives the ordinary Hamiltonian time evolution. The second, relaxation term, gives the decay of energy to the field modes. If the field is in the vacuum state the usual form of the relaxation term is

$$L[\hat{\rho}_A] = \frac{\Gamma}{2}(2\hat{C}_-\hat{\rho}_A\hat{C}_+ - \hat{C}_+\hat{C}_-\hat{\rho}_A - \hat{\rho}_A\hat{C}_+\hat{C}_-), \quad (23)$$

where Γ is the decay constant characteristic of the system. The decay operator \hat{C}_- can be $\hat{\sigma}_-$, \hat{a} , $|n\rangle\langle m|$ etc. depending on the atomic part of the system.

In quantum optics master equations of form (22) have been popular. They can be solved numerically and even analytic solutions to some simple systems are possible. If the Hilbert space of the atomic system is large, the numerical integration of the master equation takes a lot of computer memory, because density matrices must be used. In the beginning of the 1990s a new stochastic Monte Carlo wave function method was developed to integrate master equations [8, 9, 10, 11]. In this method, the

solution of the equation is obtained as an ensemble average of many stochastic time evolutions called trajectories or Monte Carlo wave functions. If the system has N basis vectors, only N complex coefficients are needed to represent a quantum state instead of N^2 required if density matrices were used. There are several different 'unravellings' depending on how the integration is done. All different methods can be connected to some measurement scheme [12]. One of the methods [8, 9] divides the time evolution into ordinary Hamiltonian and stochastic quantum jump parts. Most of the time the system evolves as determined by an effective atomic Hamiltonian. At random times, the system undergoes a quantum jump determined by the relaxation part. Typically the jump is the change of the atomic state from the excited state to the ground state. The jump can be thought to be a consequence of the detection of the photon emitted by the atomic part. Thus this jump is connected to a direct photon detection measurement.

This particular method is easy to parallelize, which is important in numerics. It is interesting to note that quite a similar approach, the quantum diffusion model, was suggested as early as 1984 by N.Gisin [13]. At that time its benefits for numerical simulations were not realized.

One weakness of master equations is that the knowledge of the quantum mechanical state of the emitted field is lost, because the field part of the Hilbert space is traced out. For example, the spectrum of the radiation must be determined using the time evolution of the atomic part, not directly from the field state.

3.2 Cascaded master equations

In the master equation (22), a photon radiated by the atom into the modes never comes back. It is possible to generalize the approach to a case where the radiation or part of it propagates to another quantum system [14, 15, 16, 17]. The system is shown in Fig. 1. System A decays to the field modes. Part of this radiation propagates through the field modes to a separate system B. System B decays to the vacuum. No radiation propagates from system B back to the system A. The Hamiltonian of the total system can be written as

$$\hat{H} = \hat{H}_A + \hat{H}_B + \hat{H}_{AR} + \hat{H}_{BR} + \hat{H}_R, \quad (24)$$

where \hat{H}_A and \hat{H}_B are Hamiltonians for the two systems and \hat{H}_R is the field Hamiltonian. The interaction Hamiltonians \hat{H}_{AR} and \hat{H}_{BR} have the form

$$\hat{H}_{AR} = i\hbar\sqrt{2\kappa_A}(\hat{a}\hat{\mathbf{E}}^\dagger(\mathbf{r}_1) - \text{h.c.}) \quad (25)$$

$$\hat{H}_{BR} = i\hbar\sqrt{2\kappa_B}(\hat{b}\hat{\mathbf{E}}^\dagger(\mathbf{r}_2) - \text{h.c.}), \quad (26)$$

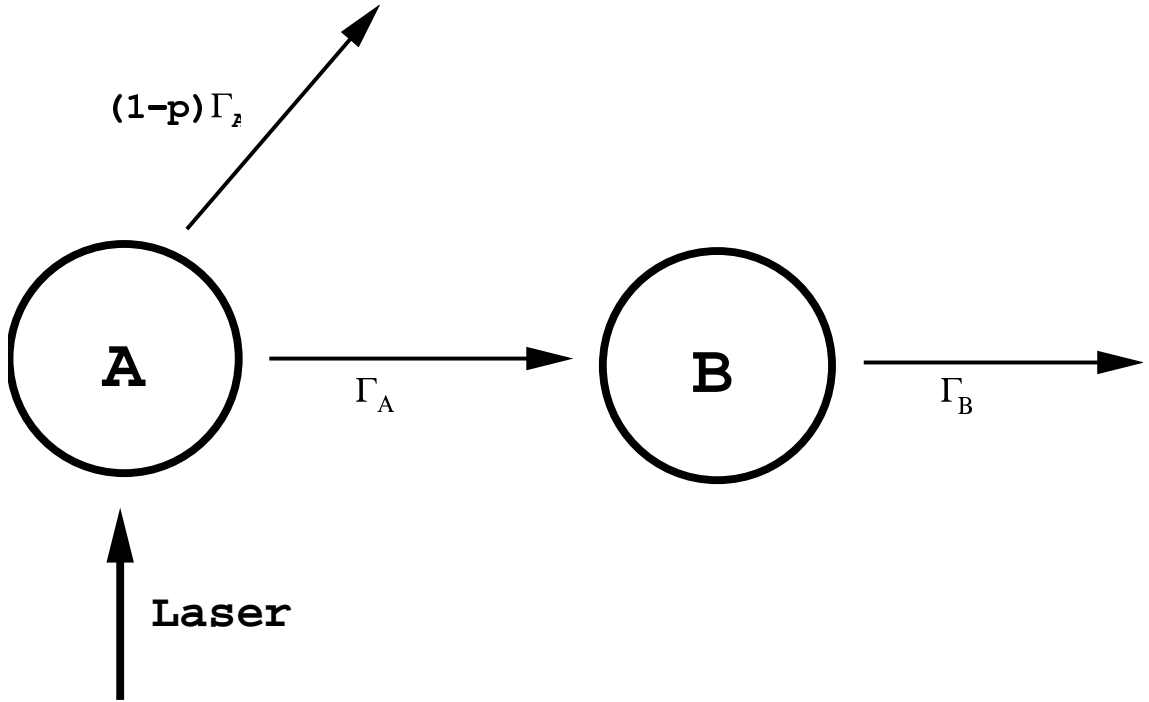


Figure 1: A cascaded open system. The system A is driven by a laser. The resonance fluorescence radiation is divided to two decay channels. The proportion p of the radiation propagates to the quantum system B. The rest of the radiation propagates directly to the field modes. Radiation from the system B propagates to the reservoir.

where the operators \hat{a} and \hat{b} are annihilation operators of the systems A and B, respectively. The interaction with the field is now at two different spatial points \mathbf{r}_1 and \mathbf{r}_2 . Using methods similar to the derivation of equation (22), it is possible to derive a master equation i.e. to trace out the field degrees of freedom. As a result we get a master equation of the familiar form

$$i\hbar \frac{d\hat{\rho}}{dt} = [\hat{H}_S, \hat{\rho}] + L[\hat{\rho}], \quad (27)$$

where

$$\hat{H}_S = \hat{H}_A + \hat{H}_B + i\hbar\sqrt{\kappa_A\kappa_B}(\hat{a}^\dagger\hat{b} - \text{h.c.}). \quad (28)$$

The term $L[\hat{\rho}]$ is the Lindblad operator

$$L[\hat{\rho}] = 2\hat{C}_-\hat{\rho}_A\hat{C}_+ - \hat{C}_+\hat{C}_-\hat{\rho}_A - \hat{\rho}_A\hat{C}_+\hat{C}_-, \quad (29)$$

with the decay operator

$$\hat{C} = \sqrt{2\kappa_A}\hat{a} + \sqrt{2\kappa_B}\hat{b}. \quad (30)$$

Because the decay term (29) has the same form as (23), the stochastic integration methods described earlier can be used. The difference in the decay constants is due to the fact that in the latter equation (29) the decay constant is for a cavity mode and in the former one (23) for the atom.

We have used the method in the first paper to compute the time dependent spectrum. In these simulations the radiation emitted from system A is detected by system B. The spectrum can be read from the quantum mechanical state of the system B. A detailed explanation is given in section 5.5.

3.3 The excitation expansion

In the derivation of a master equation, the field part of the Hilbert space is traced out. All information of the state of the field is lost. In our simulations we have used an approach in which the time evolution of the field is explicitly present. The method used is an excitation expansion around the vacuum. The basis vectors for the field are restricted to have only a few excitations. In our simulations we have allowed only a single excitation. Thus the method can be used only for fields of very small intensity. For the fields of a single excitation the general state vector has the form

$$|\Psi\rangle = \sum_{\mathbf{k}} c_{\mathbf{k}} |1\rangle_{\mathbf{k}} \prod_{\mathbf{k}' \neq \mathbf{k}} |0\rangle_{\mathbf{k}'} \equiv \sum_{\mathbf{k}} c_{\mathbf{k}} |1_{\mathbf{k}}\rangle. \quad (31)$$

The method is especially useful if the interaction Hamiltonian has the the Jaynes-Cummings form (20). For such systems, if the initial state has only one excitation, the number of basis vectors with nonzero components is restricted to a fixed number. If the field gets additional energy from the outside, this method cannot be used because basis vectors with higher excitation get nonzero coefficients. The method is restricted to very small excitation numbers because the number of basis vectors increases exponentially when the excitation number is increased.

In papers III, IV, V and VI we have also used the method in cases where there are many two-level atoms in addition to the field. The total number of excitations of basis vectors is still restricted to one. The general state vector can be written as

$$|\Psi\rangle = \sum_{\mathbf{k}} c_{\mathbf{k}} |1\rangle_{\mathbf{k}} \prod_{\mathbf{k}' \neq \mathbf{k}} |0\rangle_{\mathbf{k}'} \otimes \prod_{j=1}^{N_A} |0\rangle_j + \sum_{\mathbf{k}} |0\rangle_{\mathbf{k}} \otimes \sum_{j=1}^{N_A} c_j |1\rangle_j \prod_{j' \neq j} |0\rangle_{j'}$$

$$\equiv \sum_{\mathbf{k}} c_{\mathbf{k}} |1_{\mathbf{k}}, 0\rangle + \sum_{j=1}^{N_A} c_j |0, 1_j\rangle \quad (32)$$

where N_A is the number of the atoms. The basis functions $|0\rangle_j$ and $|1\rangle_j$ are two internal states of the j :th atom. The state vector has the same general form at later times, because of the Jaynes-Cummings interaction.

3.4 The correlation function expansion

One possible method to represent the field state might be to use correlation functions. The state of the field is determined uniquely if all the normally ordered correlation functions [4]

$$\Gamma^{(N,M)}(\mathbf{x}_1, \dots, \mathbf{x}_N; \mathbf{y}_M, \dots, \mathbf{y}_1) = \text{Tr}[\hat{\rho} \hat{F}^{(-)}(\mathbf{x}_1) \dots \hat{F}^{(-)}(\mathbf{x}_N) \hat{F}^{(+)}(\mathbf{y}_M) \dots \hat{F}^{(+)}(\mathbf{y}_1)], \quad (33)$$

where

$$\hat{F}^{(+)}(\mathbf{x}) = \frac{1}{L^{3/2}} \sum_{\mathbf{k}s} \hat{a}_{\mathbf{k}s} \epsilon_{\mathbf{k}s} e^{i(\mathbf{k}\cdot\mathbf{x} - \omega t)} \quad (34)$$

are known. The operator $\hat{F}^{(-)}(\mathbf{x})$ is the complex conjugate of $\hat{F}^{(+)}(\mathbf{x})$. The time evolution of the system is determined by coupled partial differential equations for correlation functions. For many realistic fields the first few correlations determine the field state uniquely.

Mathematically the equations of motion for the correlation functions are partial differential equations for functions of several variables. In computer simulations, the crucial point is how the functions can be represented using as little memory as possible. Thus the model demands that effective compression methods are used. There are many possibilities to compress smooth functions using as little memory as possible. One fashionable alternative is a wavelet expansion [18, 19, 20] for the functions. In order to use the method it is not necessary to determine the modes of the system. They will be implicitly taken into account in the boundary conditions of the differential equations. The method can also be used in the case when the field is coupled to atoms.

4 The stochastic harmonic oscillator

It is possible to build traps for atoms using laser light and magnetic fields. A very active field in physics is to study the properties of the atoms inside the trap. One of the greatest achievements has been the cooling of atoms to such low temperatures that a macroscopic number of atoms are in the motional ground state of the trap. Then the bosonic atoms can form a Bose-Einstein condensate [21, 22, 23, 24, 25, 26, 27, 28].

Long before the condensate research, H. Dehmelt et al. were able to trap a single electron into a magnetic trap [29, 30, 31]. They used the Penning trap [31, 32]. In this trap an electron experiences a parabolic potential. When the electron oscillates in the trap, the frequency of the oscillation depends on the direction of the electron spin. The spin can have two different values, so the frequency jumps between two different constant values. In this respect, the spin behaves like a classical observable and always has a definite value. It is possible to detect the oscillation frequency using a small coil. The coil is placed close to the oscillating electron, which induces a current into the wire. It is possible to determine the oscillation frequency by analyzing the changes in the current [33].

Because the direction of the spin can be detected continuously, the measurement is called a continuous Stern-Gerlach experiment. The times when the spin changes direction are random. Using lasers it is possible to induce different transitions between the quantum states. Using transition rates of spin flips it is possible to determine the energy differences between different states extremely accurately. The magnetic moment of an electron g_e can be determined using this data. Using quantum electrodynamics (QED) it is also possible to calculate the constant g_e . The calculated value agrees with the measured one amazingly well. H. Dehmelt was honored by the Nobel prize in Physics in 1989 for these experiments.

In paper II [34] we have developed a phenomenological model to study the time evolution of the electron. The electron experiences a stochastic potential depending on the spin direction. The Hamiltonian for its motion is

$$H = \frac{p^2}{2m} + \frac{1}{2}m\omega^2(t)x^2, \quad (35)$$

where the frequency $\omega(t)$ jumps between two different constant values stochastically. We have used two different models to determine the jumping times. In the first model the probability for a spin flip is constant $\nu\Delta t$ in a small time interval Δt . The frequency ν is the flip frequency. The main problem with this approach is that the electron absorbs a lot of energy and in realistic experiment would escape from the trap. The reason for this is that the jumps occur near the turning points where the electron is most of the

time. In order to avoid this we have used another method to get the flip times. Instead of a constant we take the jump probability from state one to state two to be

$$P_{12}(t) = \nu |\langle \Psi_2^0 | \Psi_1(t) \rangle|^2, \quad (36)$$

where Ψ_2^0 is the ground state wave function of the potential with frequency ω_2 . The probability for a jump from state 2 to state 1 is obtained by interchanging the labels 1 and 2. This choice of the jump probability favors jumps in the center of the trap and thus the energy absorption is not a big problem. The stochastic models used here are purely phenomenological and not the same as used in the integration of master equations in Sec. 3.1.

The initial state of the electron used in our simulations is a Gaussian

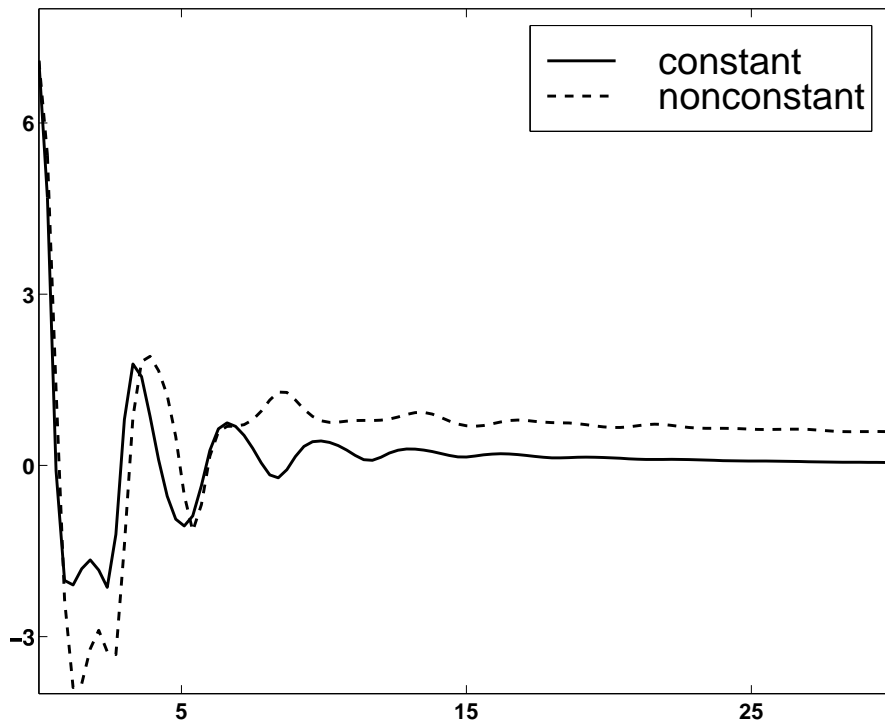


Figure 2: The time evolution of the x -coherence (39) as a function of time. In the beginning when the system is in the pure state the coherence has an oscillating behavior. The oscillations are damped at later times. At large time values, the density matrix in the case of a constant jump probability becomes diagonal i.e. the coherence is lost. In the nonconstant case there is a finite coherence asymptotically.

$$\Psi(x) = (2\pi\sigma_x^2)^{-1/4} \exp\left(-\frac{(x - \langle x \rangle)^2}{4\sigma_x^2} + \frac{i\sigma_{xp}^2}{2\hbar\sigma_x^2}(x - \langle x \rangle)^2 + \frac{i\langle p \rangle}{\hbar}(x - \langle x \rangle) + i\theta\right). \quad (37)$$

Parameters $\langle x \rangle$ and $\langle p \rangle$ are expectation values of position and momentum. Parameters $\sigma_x^2 = \langle x^2 \rangle - \langle x \rangle^2$ and $\sigma_p^2 = \langle p^2 \rangle - \langle p \rangle^2$ are the variances of position and momentum. The cross variance is defined as $\sigma_{xp}^2 = \langle xp \rangle - \langle x \rangle \langle p \rangle$. The expectation value $\langle xp \rangle$ is calculated using the symmetric operator ordering $\langle xp \rangle = \frac{1}{2}(\langle \hat{x}\hat{p} \rangle + \langle \hat{p}\hat{x} \rangle)$. The variances are not all independent, they satisfy the relation

$$\sigma_x^2\sigma_p^2 - (\sigma_{xp}^2)^2 = \frac{\hbar^2}{4}. \quad (38)$$

The parameter θ is a phase factor. Because the potential part of the Hamiltonian (35) is harmonic, the state vector preserves its Gaussian form. The time evolution reduces to the time evolution of the parameters $\langle x \rangle$, $\langle p \rangle$, σ_x^2 , σ_p^2 , σ_{xp}^2 and θ . We have calculated several ensemble expectation values using constant and non-constant jump frequencies described above.

As mentioned earlier, the energy the electron absorbs when a constant jump potential is used increases exponentially. For a non-constant case the absorption is much slower. The oscillation of the ensemble momentum and position is damped faster with the non-constant jump probability. The off-diagonal elements of the ensemble density matrix get smaller. When the jump probability is constant the value of the spatial coherence

$$\langle x^2 \rangle = \int \int dx_1 dx_2 (x_1 - x_2)^2 \langle x_1 | \hat{\rho} | x_2 \rangle \quad (39)$$

disappears as seen in Fig. 2. In the non-constant case the coherence does not disappear completely. The diagonal elements of the density matrix $\langle n | \hat{\rho} | n \rangle$ approach a thermal distribution, Fig. 3. It can be seen that in the case of the constant jump probability more energy is absorbed. In paper II we have also studied the situations where the initial state has a squeezed Gaussian form. The essential results are the same as described above.

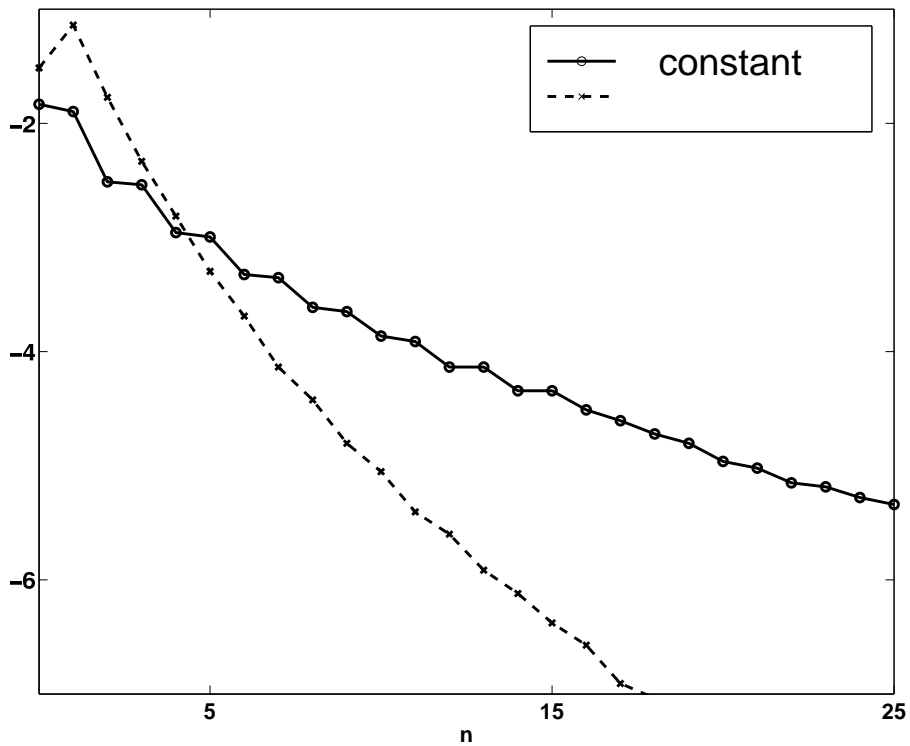


Figure 3: The diagonal elements of the density matrix of the electron in the Fock representation $\langle n | \hat{\rho} | n \rangle$ at large time value. The scale of the y -axis is logarithmic, so the distribution is exponential. It is seen that with a constant jump probability the elements with bigger n have more excitation than in the non-constant case. Thus the electron absorbs more energy and is heated.

5 The spectrum of the radiation field

5.1 Mode spectrum

Every radiation field has some characteristic frequency distribution, a spectrum. For the review of different definitions of spectrum see the paper by J. D. Cresser [35]. If canonical quantization is used, the spectrum of the field in the whole quantization volume can be defined using the expectation value of the number operator $\hat{n}_{\mathbf{k}s} = \hat{a}_{\mathbf{k}s}^\dagger \hat{a}_{\mathbf{k}s}$. The spectrum is the sum of the expectation values of the number operators at a specific frequency

$$S(\omega) \propto \int \sum_s \delta(\omega - \omega_{\mathbf{k}}) \langle \hat{n}_{\mathbf{k}s} \rangle d^3k, \quad (40)$$

where the expectation value is taken with the general state (16). This gives the *nonlocal, time dependent* spectrum of the field in the cavity. For any realistic measurement it is impossible to measure the spectrum of the field in the whole cavity at a given time, so one might think that the formula (40) is only of theoretical interest.

However, it is possible to restrict the mode spectrum to a smaller region. One method is to calculate all correlation functions of the field. Because they are functions of position, they can be used to filter the radiation in such a way that the determination of a more local mode spectrum is possible. All values of correlation functions with spatial coordinates outside of the given region are filtered to zero. Correlations with coordinates inside the region are unchanged. The expectation value of $\hat{n}_{\mathbf{k}s}$ in equation (40) is calculated using the filtered field. The resulting spectrum is the mode spectrum of the field inside a filtered region.

5.2 Fourier spectrum

A common situation is that the state of the field is traced out and is not available. Thus the calculation of the mode spectrum is not possible. Then the time evolution of the system is described by a master equation. For stationary fields the usual definition of the spectrum is

$$S(\omega) = \int_{-\infty}^{\infty} d\tau \langle \hat{\mathbf{E}}^-(t + \tau) \cdot \hat{\mathbf{E}}^+(t) \rangle e^{i\omega\tau}, \quad (41)$$

i.e. the Fourier transform of a normally ordered two time average. The field is stationary if correlation functions of the field are invariant under displacements of

the time variable, for example the value of the second order correlation function $\langle \hat{\mathbf{E}}(\mathbf{r}_1, t_1) \cdot \hat{\mathbf{E}}(\mathbf{r}_2, t_2) \rangle$ depends only on the time difference $\tau = t_2 - t_1$. If master equations are used, the definition can be written for the two time average of the system operators, for example $\hat{\mathbf{E}}^\pm \propto \hat{\sigma}_\pm$. It is not straightforward to see how to calculate two time averages using master equations. The method to do it, the quantum regression theorem (QRT) [5, 8] was first given by Lax in 1963 [36], as a generalization of the classical result by Onsager [37]. It is also possible to determine two time averages using the Monte Carlo wave function approach [10, 38, 39].

There are many problems with the spectrum defined by (41). First of all it is defined only for stationary fields. In nature there are no fields which are truly stationary. The measurement scheme which is essential in quantum optics is not taken into account in the definition. One can say that it is really surprising that equation (41) gives something which is related to a measured spectrum. The criticism of the Fourier spectrum is not new and there has been many suggestions for spectra of nonstationary fields.

5.3 Generalizations of Fourier spectrum

One generalization of the Fourier spectrum has been suggested by Page and Lampard [40, 41]. They define the spectrum as

$$G_{PL}(\omega, t) = \int_{-\infty}^{\infty} d\tau \left[\langle \hat{\mathbf{E}}^-(t) \hat{\mathbf{E}}^+(t - \tau) \rangle \theta(\tau) + \langle \hat{\mathbf{E}}^-(t + \tau) \hat{\mathbf{E}}^+(t) \rangle \theta(-\tau) \right], \quad (42)$$

where $\theta(\tau)$ is the step function

$$\theta(\tau) = \begin{cases} 1, & \tau \geq 0 \\ 0, & \tau < 0. \end{cases} \quad (43)$$

The spectrum (42) is time dependent and defined also for nonstationary fields. The integral is restricted to correlation functions in which time values are less than the time t , so the future evolution of the field does not affect the spectrum. For a stationary field the definition (42) gives the Fourier spectrum. However, the Page-Lampard spectrum has some weaknesses, for example it may be negative.

Another generalization was suggested by Silverman [42]. He considers a two time integral

$$\Psi(\omega, \omega') = \int_{-\infty}^{\infty} dt \int_{-\infty}^{\infty} dt' e^{i(\omega t - \omega' t')} \langle \hat{\mathbf{E}}^-(t) \hat{\mathbf{E}}^+(t') \rangle. \quad (44)$$

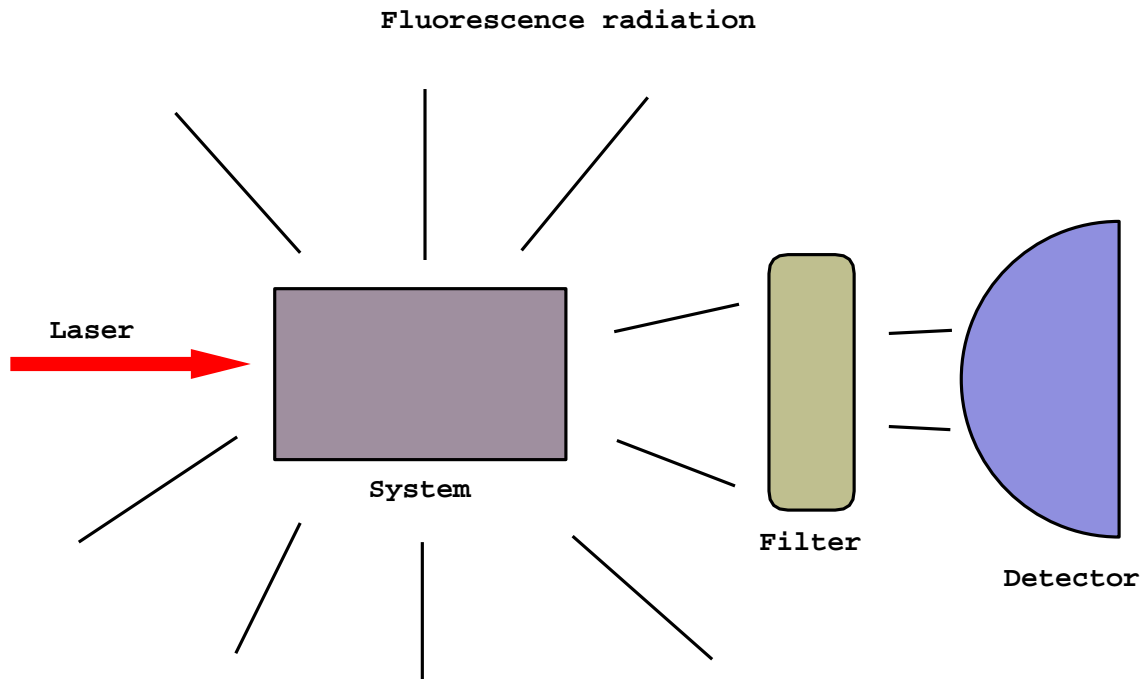


Figure 4: A configuration of a realistic spectrum measurement. The system which might be driven by a laser emits fluorescence radiation. In front of the intensity detector there is a frequency sensitive filter. It allows radiation at a specific tunable frequency to go through it. The spectrum is obtained from the relative intensities detected by the detector at different frequencies.

The spectrum (44) has been used for locally stationary processes, where the time evolution of the field can be divided into fast and slowly evolving parts. For a stationary field it reduces to a Fourier spectrum. One problem is that it depends on future values of the field and for a general field this is not physical.

5.4 Physical spectrum

Eberly and Wódkiewicz have suggested a spectrum [43, 44] which takes the measurement scheme into account. A typical spectrum measurement is shown in Fig. 4. The radiation from the system is detected at the intensity detector. In front of the detector there is a tunable filter, which can be characterized by a frequency ω_f and a width Γ_f . The filter allows the radiation with a frequency close to ω_f to pass to the detector.

The filter function is centered at ω_f with the characteristic width Γ_f . The measured spectrum is obtained as an appropriately normalized intensity measured at the detector as the filter is tuned over different frequencies ω_f . The spectrum is obviously time dependent and it can be measured for all kinds of fields. Mathematically the spectrum of the field which reaches the detector is

$$\hat{\mathbf{E}}_D(\omega, t) = H(\omega, \omega_f, \Gamma_f) \hat{\mathbf{E}}(\omega, t), \quad (45)$$

where $H(\omega, \omega_f, \Gamma_f)$ is the filter function. In time the relation (45) becomes

$$\hat{\mathbf{E}}(t) = \int_{-\infty}^{\infty} dt' H(t - t', \omega_f, \Gamma_f) \hat{\mathbf{E}}(t'), \quad (46)$$

where $H(t - t', \omega_f, \Gamma_f)$ is the Fourier transform of the filter function in frequency space. The counting rate at the detector is

$$S(t, \omega) = \int_{-\infty}^{\infty} dt_1 \int_{-\infty}^{\infty} dt_2 H^*(t - t_1, \omega_f, \Gamma_f) H(t - t_2, \omega_f, \Gamma_f) \langle \hat{\mathbf{E}}^-(t_1) \hat{\mathbf{E}}^+(t_2) \rangle. \quad (47)$$

The filter function for a Fabry-Perot filter is

$$H(t, \omega_f, \Gamma_f) = \theta(t) \Gamma_f e^{-(\Gamma_f + i\omega_f)t}, \quad (48)$$

and this gives

$$S(t, \omega_f, \Gamma_f) = \Gamma_f^2 \int_{-\infty}^t dt_1 \int_{-\infty}^t dt_2 e^{-(\Gamma_f - i\omega_f)(t-t_1)} e^{-(\Gamma_f + i\omega_f)(t-t_2)} \langle \hat{\mathbf{E}}^-(t_1) \hat{\mathbf{E}}^+(t_2) \rangle. \quad (49)$$

For a stationary field, the definition (49) reduces to the Fourier spectrum if the filter is ideal ($\Gamma_f \rightarrow 0$). The method to get time dependence into the spectrum is similar to the method which was used to get spatial dependence into the mode spectrum. In both cases, filter function, which restricts the correlations taken into account, is introduced.

5.5 Analyser atom spectrum

It is possible to use the theory of cascaded open systems to model both the filter and the detector in the measurement scheme. The detailed explanation of the method can

be found in paper I[45]. The configuration is the same as in Fig. 1. The radiation from a system A is divided into two parts. A very small fraction p goes to system B, which is a set of two-level atoms. Most of the radiation goes into other directions. All atoms have very small, identical decay constants. The frequencies are all different

$$\omega_n = \omega_{min} + n \cdot \Delta\omega, \quad n = 1, 2, 3 \dots N, \quad \Delta\omega = \frac{\omega_{max} - \omega_{min}}{N - 1}. \quad (50)$$

All atoms are initially in the ground state. Because their line widths are small, only radiation which is exactly on resonance can excite an atom. The excitation probability is directly proportional to the intensity of the radiation at the resonance frequency. The appropriately normalized atomic excitation as a function of frequency gives the time dependent spectrum of the radiation.

We have used the atoms as a mathematical model to determine the spectrum. It might be possible to realize the measurement using atoms which are guided through the radiation field. Different resonance frequencies are obtained using an appropriate magnetic field. After the atoms have passed the radiation of interest, the intensity of the radiation which comes from the atomic decay is measured. The relative intensity gives the spectrum.

The method is closely related to a measurement scheme and can be used for all kinds of physical systems. In paper I we have used the method to determine the resonance fluorescence spectrum of a laser driven three-level atom. The results were identical to the physical spectrum defined by equation (49). In paper V the method was used for the radiation in a one-dimensional cavity. The result was identical to the local mode spectrum determined using filtered correlation functions. We emphasize that the benefit of the method of analyzer atoms to determine the spectrum is that only one time averages are used. Thus the quantum regression theorem is not needed.

6 Cavity QED simulations in 1D

In the previous section we showed how a group of two-level atoms can be used to determine the spectrum of the field. The measurement system was treated using a cascaded master equation. We have also used the method in one-dimensional cavity QED simulations where the state of the field is followed explicitly (paper V). In these simulations we used one-dimensional cavities [46, 47, 48]. Inside the cavity there are N_A two-level atoms which are coupled to the radiation field through a dipole coupling. The state of the field is restricted to have only one excitation. There are two mirrors at the edges of the cavity ($x = 0, L$). The field can be expanded using basis functions

$$\begin{aligned}\hat{E}(r) &= \sum_{n=1}^{\infty} \left(\frac{\hbar\omega_n}{\epsilon_0 L} \right)^{1/2} \sin(k_n r) (\hat{a}_n + \hat{a}_n^\dagger), \\ \hat{B}(r) &= i \sum_{n=1}^{\infty} \left(\frac{\hbar\omega_n \mu_0}{L} \right)^{1/2} \sin(k_n r) (\hat{a}_n - \hat{a}_n^\dagger).\end{aligned}\tag{51}$$

Basis vectors of the system can be divided into field and atomic parts. The general state vector with one excitation is

$$|\Psi\rangle = \sum_{n=1}^{\infty} (c_n |1\rangle_n \prod_{n' \neq n} |0\rangle_{n'}) \otimes \prod_{j=1}^{N_A} |0\rangle_j + \sum_{n=1}^{\infty} |0\rangle_n \otimes \sum_{j=1}^{N_A} (c_j |1\rangle_j \prod_{j' \neq j} |0\rangle_{j'})\tag{52}$$

$$\equiv \sum_{n=1}^{\infty} c_n |1_n, 0\rangle + \sum_{j=1}^{N_A} c_j |0, 1_j\rangle.\tag{53}$$

In the first term one of the modes has the excitation and in the second term one atom is excited. The Hamiltonians for the system are

$$\hat{H}_F = \sum_{n=1}^{\infty} \hbar\omega_n \hat{a}_n^\dagger \hat{a}_n,\tag{54}$$

$$\hat{H}_A = \frac{\hbar}{2} \sum_{j=1}^{N_A} \omega_j \hat{\sigma}_z^j,\tag{55}$$

$$\hat{H}_I = -\hbar \sum_{j=1}^{N_A} \sum_{n=1}^{\infty} g_n^j (\hat{a}_n \hat{\sigma}_+^j + \hat{a}_n^\dagger \hat{\sigma}_-^j),\tag{56}$$

where the coupling coefficient g_n^j is

$$g_n^j = \left(\frac{\omega_n}{\hbar \epsilon_0 L} \right)^{1/2} D_j \sin(k_n r_j). \quad (57)$$

The vacuum energy has been left out from the field Hamiltonian. The operators $\hat{\sigma}^j$ are the Pauli spin matrices for the atoms. In the interaction Hamiltonian, dipole and rotating wave approximations (RWA) have been used.

The two-level atoms are used to detect the spectrum in several simulations. In the first simulation, Fig. 5, there is one atom at the center of the cavity. The field,

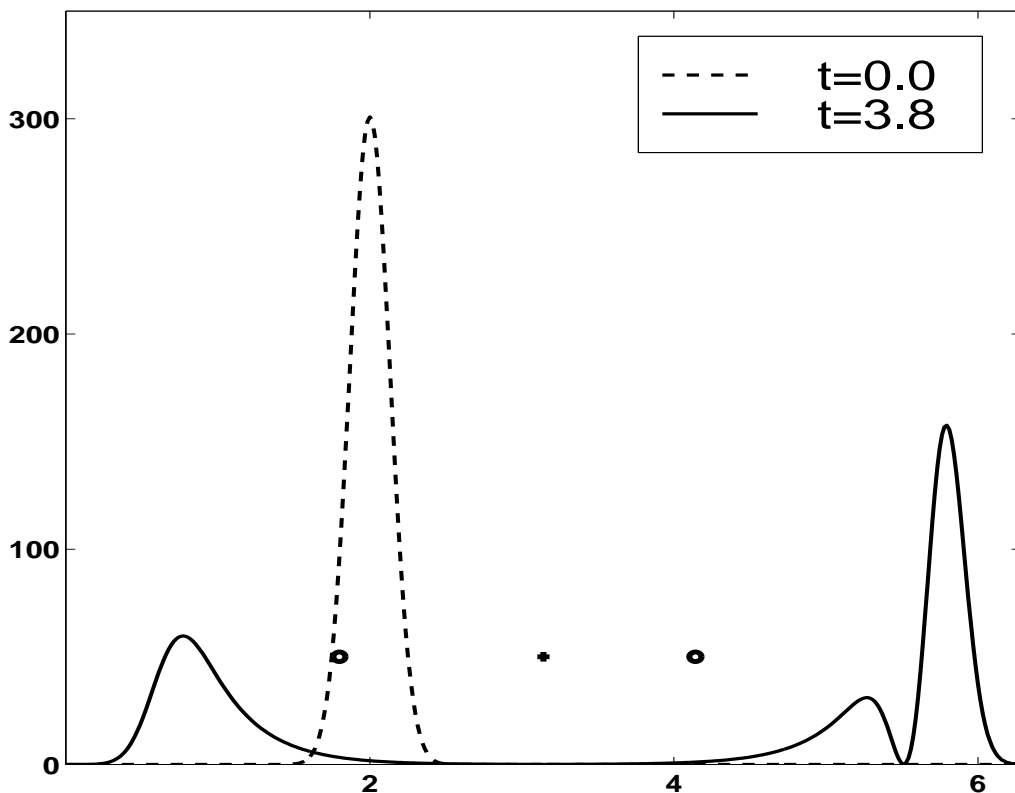


Figure 5: The intensity of the radiation field at two different times. At the center there is one atom which interacts with the field. To the left and right from the center (little circles), there are analyser atoms which detect the spectrum of the field which passes them. At $t = 0.0$ the photon propagates to the right. At $t = 3.8$ part of the radiation has reflected to the left and part has passed the atom and propagates to the right.

which has a Gaussian distribution in k -space (mode spectrum), propagates to the right towards the center atom. The resonance frequency of the center atom is on resonance with the incoming radiation. The linewidth of the atom Γ_A is smaller than the width of the initial photon Γ_{ph} . To the right and left from the center, there are two level atoms which detect the spectrum as was described in Section 5.5. The spectrum is read from the excitation probabilities of the analyser atoms at a specific time.

The center atom splits the field into left and right propagating parts. The field on the right has two peaks and on the left only one peak. The first peak on the right is a part of the initial photon which do not interact with the atom. The second peak is a result of the atomic decay. We have measured the spectra of the two peaks on the right separately using analyser atoms with time dependent dipole constants. The dipole constants of the analyser atoms which detect the spectrum of the second peak are switched on after the first peak has passed them. The spectra are shown in Fig. 6. Both are peak-like spectra and the spectrum of the second peak is narrower. This is easy to understand, because the intensity profile of the second peak is wider and it interacts with the atoms longer. According to the uncertainty principle the longer the interaction time between two systems is the smaller details can be seen in the spectrum. The intensity profile of the second peak is wider because the atomic linewidth is smaller than the width of the initial photon $\Gamma_A < \Gamma_{ph}$. Had we chosen the other case $\Gamma_A > \Gamma_{ph}$ the first intensity peak would be wider than the second. The measured spectra would be different too. The spectrum on the left has a similar peak, Fig. 7.

The spectrum of the total intensity on the right is shown in Fig. 7. The original Gaussian profile has a hole in the middle. The resonant radiation has been reflected and off-resonant radiation has passed the atom. When the spectrum of the total intensity on the right is measured, there is no radiation at the resonance frequency. On the other hand spectra of the two intensity peaks measured separately both had a peak like spectrum centered at the resonance frequency. This shows nicely that the spectrum is not additive. The second peak creates a stimulated emission type of effect which decreases the excitations of atoms with resonance frequencies.

We have compared the spectra measured by the atoms with the local mode spectrum, which was calculated using the methods described in Section 5.1. In order to get the mode spectrum we first calculate the first order correlation function $g(r_1, r_2, t) = \langle \hat{\mathbf{E}}^-(r_1, t) \hat{\mathbf{E}}^+(r_2, t) \rangle$ of the field. The state vector of the field (52) is uniquely determined if the correlation $g(r_1, r_2, t)$ is known, so it is possible to calculate the coefficients c_i in equation (52). The mode spectrum in this case is given by the absolute values of the coefficients $|c_i|^2$. Using filter functions it is possible to get spatial information about the spectrum. If the correlation function $g(r_1, r_2, t)$ is filtered in such a way that only the left ($r_1, r_2 < \frac{L}{2}$) or right ($r_1, r_2 > \frac{L}{2}$) part is nonzero and the mode spectrum $|c_i|^2$ is

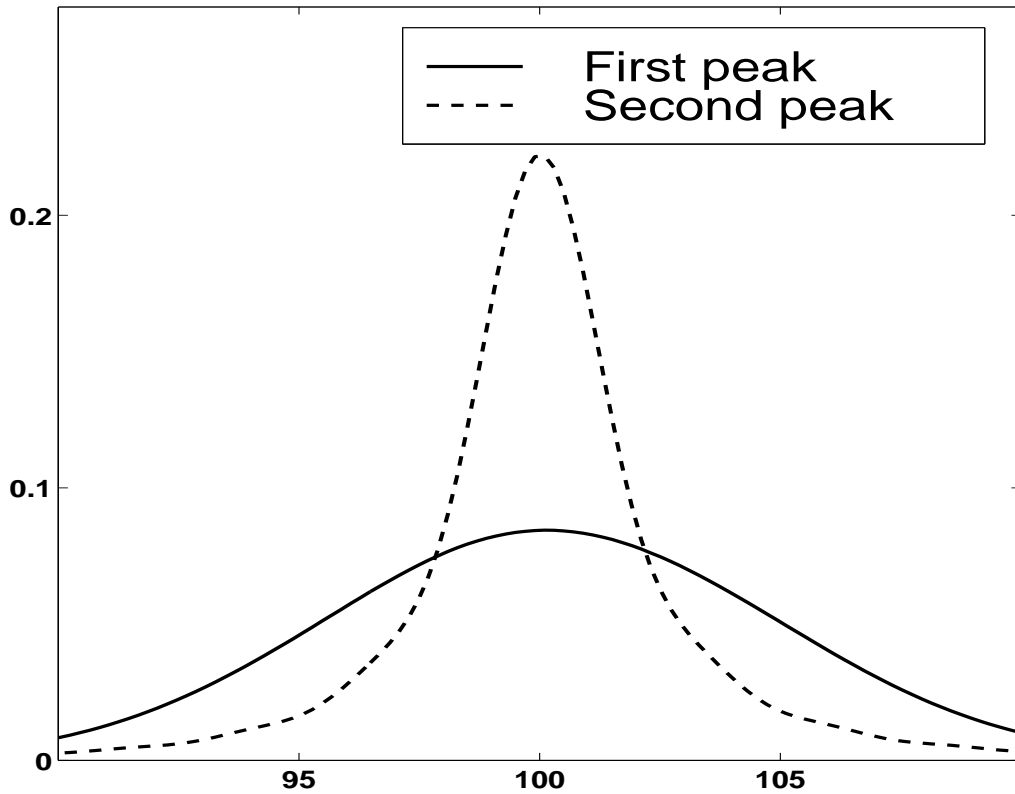


Figure 6: The spectra of the two peaks on the right in the Fig. 5, measured separately using analyser atoms with time dependent coupling constants. The spectrum of the second peak is narrower and its intensity profile is wider, Fig. 5. This is because the linewidth of the atom is smaller than the width of the initial photon. The spectrum of the initial photon is similar to the spectrum of the first peak. Both spectra have been normalized to have a unit area.

calculated, using this correlation function we get the spectrum of the radiation on the left and right respectively. The spectra calculated using filtered correlation functions give exactly the same results as measured by analyser atoms, Fig. 7.

We have used the method also in the case when there are three atoms with different resonance frequencies in the center. One of the atoms has a smaller decay constant Γ , than the two others. The spectra detected on the left and right are shown in Fig. 8. The radiation which is on resonance is reflected and off-resonance radiation has passed the atoms. So the behavior is exactly the same as in the single atom simulation. The peak with the largest frequency is narrower because the decay constant is smaller. Again the filtered correlation function gives the same results. When the spectrum of radiation is determined using filtered correlation functions or analyser atoms, two time averages are not needed. It is known that the usual method to calculate two time averages, the quantum regression theorem, gives incorrect results if the interaction between the field and the atoms is strong [49]. It would be interesting to compare the spectra obtained using different methods in this kind of situations.

The two-level atoms can also be used to model a dielectric crystal. In paper III we have studied the spontaneous emission inside a dielectric. The decaying atom is in the middle of two-level atoms. The configuration of crystal atoms affects the decay. Regular spacing between the atoms is a model for material lattice. We have also used random distances between the atoms. This would correspond to decay in an amorphous material. The generic behavior is that the decay inside a material is slower than in the free space.

In the same paper we have studied the decay of an atom near the cavity mirrors. The mirror affects the decay significantly. The decay of the atom near the mirror can be faster or slower depending on the distance from the mirror. Another problem we have studied is the propagation of radiation through a crystal of two-level atoms. We have analyzed the spectrum of the radiation which passes the crystal and the general result is the same as in the simulations with only one or a few atoms. The radiation which is on resonance with the atoms is reflected and absorbed in the crystal and the off-resonant radiation passes the crystal without interaction.

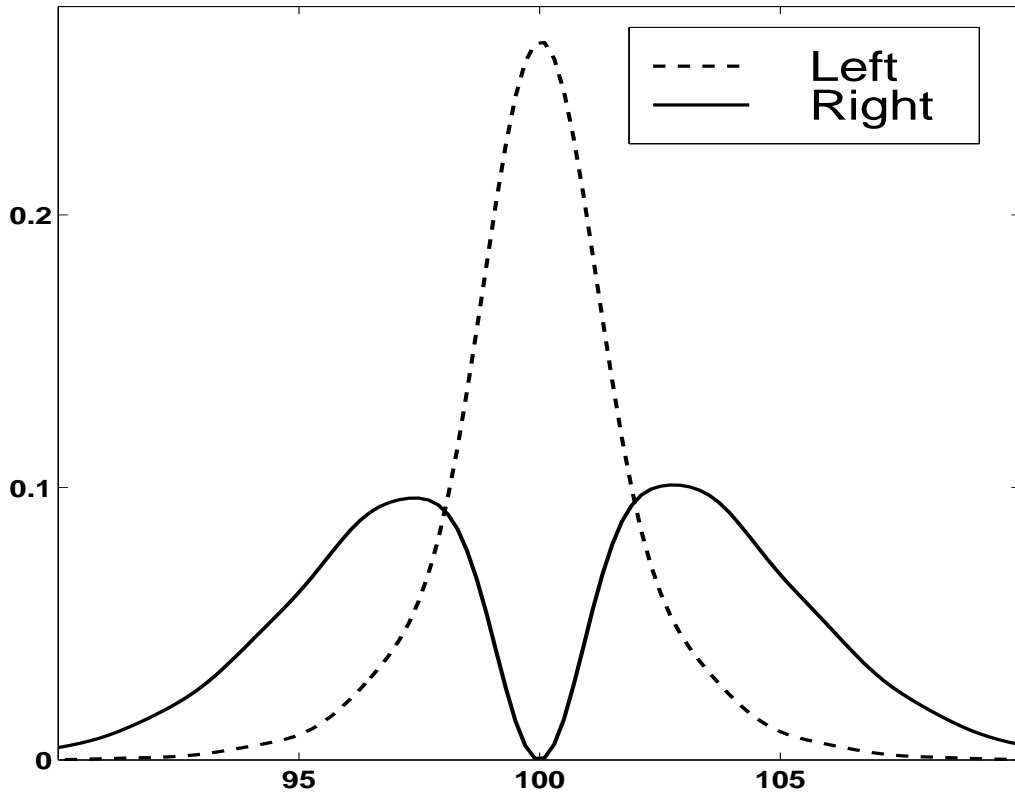


Figure 7: Spectrum of the total intensity on the right and left in Fig. 5. The resonant radiation has reflected to the left and has only one peak. The radiation on the right (two peaks) has a hole at the resonance frequency. The hole is a result of the second peak. It creates a stimulated emission type of effect and the excitations of atoms with resonance frequencies decreases. The spectra of the two intensity peaks measured separately had only one peak, Fig. 6. Normalization of the spectra is the same as in Fig. 6.

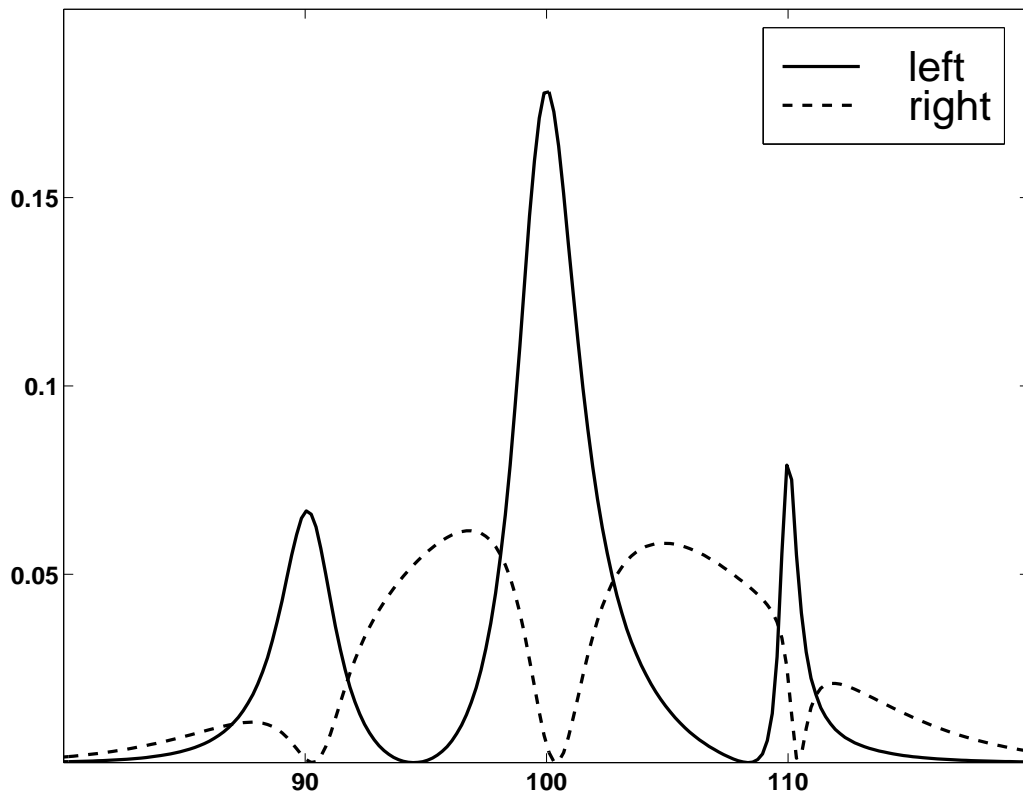


Figure 8: Spectra of the radiation on the left and right when there are three atoms in the center. The radiation at the resonance frequencies has been reflected and the off-resonance radiation has passed by the atoms. The width of the peak (or hole) at $\omega = 110$ is narrower than those of the two other peaks because its decay constant is smaller.

7 Cavity QED simulations in 2D

7.1 The general theory

In paper IV we show that it is possible to generalize the model used in the last section to two dimensions [50]. In one-dimensional simulations we used vanishing boundary conditions at the mirrors. In two dimensions, periodic boundary conditions are chosen. If some of the field energy propagates to the right edge of the cavity it will reappear from the left. This is of course unphysical, and in realistic situations we must avoid that kind of behavior. As in the one dimensional case, there are two-level atoms inside the cavity. As we will see, it is possible to build many complicated structures, for example mirrors and beam splitters using atoms.

The general state vector is again restricted to have only one excitation:

$$|\Psi\rangle = \sum_{\mathbf{k}} \left(c_{\mathbf{k}} |1\rangle_{\mathbf{k}} \prod_{\mathbf{k}' \neq \mathbf{k}} |0\rangle_{\mathbf{k}'} \right) \otimes \prod_{j=1}^{N_A} |0\rangle_j + \sum_{\mathbf{k}} |0\rangle_{\mathbf{k}} \otimes \sum_{j=1}^{N_A} \left(c_j |1\rangle_j \prod_{j'=1, j' \neq j}^{N_A} |0\rangle_{j'} \right) \quad (58)$$

$$= \sum_{\mathbf{k}} c_{\mathbf{k}} |1_{\mathbf{k}}, \{0\}\rangle + \sum_{j=1}^{N_A} c_j |\{0\}, 1_j\rangle. \quad (59)$$

We consider the radiation with a definite polarization, so the polarization index is not included in the sum. The Hamiltonians generalizing the one-dimensional case are

$$\hat{H}_F = \sum_{\mathbf{k}} \hbar \omega_{\mathbf{k}} \hat{a}_{\mathbf{k}}^\dagger \hat{a}_{\mathbf{k}}, \quad (60)$$

$$\hat{H}_A = \sum_{j=1}^{N_A} \hbar \omega_j \hat{\sigma}_z^j, \quad (61)$$

$$\hat{H}_I = \sum_{j=1}^{N_A} \sum_{\mathbf{k}} \left(g(j, \mathbf{k}) \hat{\sigma}_+^j \hat{a}_{\mathbf{k}} + g^*(j, \mathbf{k}) \hat{\sigma}_-^j \hat{a}_{\mathbf{k}}^\dagger \right) = \hat{H}_{I1} + \hat{H}_{I2}, \quad (62)$$

where the coupling constant is

$$g(j, \mathbf{k}) = -\frac{i\hbar}{2\epsilon_0 L} \sqrt{\omega_{\mathbf{k}}} D_j e^{i\mathbf{k} \cdot \mathbf{r}_j}. \quad (63)$$

As in the one-dimensional case, the dipole and rotating wave approximations have been introduced in the interaction Hamiltonian.

In two dimensions there is an additional problem related to the efficiency of the numerical simulations. In the simulations the operation $\hat{H}|\Psi\rangle$ is used extensively. In one dimension direct multiplication of matrix elements was used. However, in two dimensions this would be too slow, especially if the number of atoms inside the cavity is large. It is faster to do the simulations in the interaction picture. The state vectors and the interaction Hamiltonian is transformed according to

$$|\Psi\rangle^{(I)} = \exp(i(\hat{H}_F + \hat{H}_A)t/\hbar)|\Psi\rangle = \sum_{\mathbf{k}} c_{\mathbf{k}} e^{i\omega_{\mathbf{k}}t} |1_{\mathbf{k}}, \{0\}\rangle + \sum_{j=1}^{N_A} c_j e^{i\omega_j t} |\{0\}, 1_j\rangle \quad (64)$$

and

$$\hat{H}_I^{(I)} = \exp(i(\hat{H}_F + \hat{H}_A)t/\hbar) \hat{H}_I \exp(-i(\hat{H}_F + \hat{H}_A)t/\hbar) \quad (65)$$

$$= \sum_{j=1}^{N_A} \sum_{\mathbf{k}} \left(g(j, \mathbf{k}) e^{i(\omega_j - \omega_{\mathbf{k}})t} \hat{\sigma}_+^j \hat{a}_{\mathbf{k}} + g^*(j, \mathbf{k}) e^{-i(\omega_j - \omega_{\mathbf{k}})t} \hat{\sigma}_-^j \hat{a}_{\mathbf{k}}^\dagger \right) \quad (66)$$

$$= \hat{H}_{I1}^{(I)} + \hat{H}_{I2}^{(I)}. \quad (67)$$

The operation of the two parts of the interaction Hamiltonian on the state vector (64) gives

$$\begin{aligned} \hat{H}_{I1}^{(I)} |1_{\mathbf{k}}, \{0\}\rangle^{(I)} &= -\frac{i\hbar}{2\epsilon_0 L} \sum_{j=1}^{N_A} \sum_{\mathbf{k}'} \sqrt{\omega_{\mathbf{k}'}} D_j e^{i\mathbf{k}' \cdot \mathbf{r}_j} e^{i(\omega_j - \omega_{\mathbf{k}})t} \hat{\sigma}_+^j \hat{a}_{\mathbf{k}'} |1_{\mathbf{k}}, \{0\}\rangle \\ &= -\frac{i\hbar}{2\epsilon_0 L} \sum_{j=1}^{N_A} \sqrt{\omega_{\mathbf{k}}} D_j e^{i\mathbf{k} \cdot \mathbf{r}_j} e^{i(\omega_j - \omega_{\mathbf{k}})t} |\{0\}, 1_j\rangle \end{aligned} \quad (68)$$

$$\hat{H}_{I1}^{(I)} |\{0\}, 1_l\rangle^{(I)} = 0, \quad l = 1 \dots N_A, \quad (69)$$

$$\hat{H}_{I2}^{(I)} |1_{\mathbf{k}}, \{0\}\rangle^{(I)} = 0, \quad (70)$$

$$\begin{aligned} \hat{H}_{I2}^{(I)} |\{0\}, 1_l\rangle^{(I)} &= \frac{i\hbar}{2\epsilon_0 L} \sum_{j=1}^{N_A} \sum_{\mathbf{k}} \sqrt{\omega_{\mathbf{k}}} D_j^* e^{-i\mathbf{k} \cdot \mathbf{r}_j} e^{-i(\omega_j - \omega_{\mathbf{k}})t} \hat{\sigma}_-^j \hat{a}_{\mathbf{k}}^\dagger |\{0\}, 1_l\rangle \\ &= \frac{i\hbar}{2\epsilon_0 L} \sum_{\mathbf{k}} \sqrt{\omega_{\mathbf{k}}} D_l^* e^{-i\mathbf{k} \cdot \mathbf{r}_l} e^{-i(\omega_l - \omega_{\mathbf{k}})t} |1_{\mathbf{k}}, \{0\}\rangle, \quad l = 1 \dots N_A. \end{aligned} \quad (71)$$

The new coefficients of the state vector $\hat{H}_I^{(I)}|\Psi\rangle$, which is of the form (59), are

$$c'_j = -\frac{i\hbar}{2\epsilon_0 L} D_j e^{i\omega_j t} T(\mathbf{r}_j, t), \quad (72)$$

$$c'_\mathbf{k} = \frac{i\hbar}{2\epsilon_0 L} e^{i\omega_\mathbf{k} t} U(\mathbf{k}, t), \quad (73)$$

where

$$T(\mathbf{r}, t) = \sum_{\mathbf{k}} \left(c_{\mathbf{k}} \sqrt{\omega_{\mathbf{k}}} e^{-i\omega_{\mathbf{k}} t} \right) e^{i\mathbf{k} \cdot \mathbf{r}}, \quad (74)$$

$$U(\mathbf{k}, t) = \sum_{\mathbf{r}} \left(\sum_{j=1}^{N_A} \sqrt{\omega_{\mathbf{k}}} D_j^* c_j \delta(\mathbf{r} - \mathbf{r}_j) e^{-i\omega_j t} \right) e^{-i\mathbf{k} \cdot \mathbf{r}}. \quad (75)$$

It is seen that both terms (74) and (75) are two dimensional Fourier transforms over \mathbf{k} and configuration spaces respectively. This is important because now in numerical simulations the Fast Fourier Transform (FFT) can be used. This makes some simulations orders of magnitude faster and allows us to simulate atomic configurations which would be impossible without FFT.

7.2 Various simulations

Next we show how two-level atoms can be used to build mirrors and beam splitters. These can form the basis to build complicated optical networks. Mirrors may have an arbitrary shape. We have carried out simulations with plane and parabolic mirrors. Circular and square mirrors are used to build closed cavities.

7.2.1 A free photon

First we show the time evolution of a free photon. There are no atoms inside the cavity. The initial state of the field used in many simulations is a product of two one-dimensional Gaussian distributions

$$|\Psi\rangle = \sum_{\mathbf{k}} c_{\mathbf{k}} |1_{\mathbf{k}}, \{0\}\rangle, \quad (76)$$

where the mode coefficient $c_{\mathbf{k}}$ is

$$c_{\mathbf{k}} = (2\pi\Delta_{k_x}^2)^{-1/4} (2\pi\Delta_{k_y}^2)^{-1/4} e^{-i\mathbf{k} \cdot \mathbf{r}_0} \exp\left(-\frac{(k_x - k_{x0})^2}{4\Delta_{k_x}^2} - \frac{(k_y - k_{y0})^2}{4\Delta_{k_y}^2}\right). \quad (77)$$

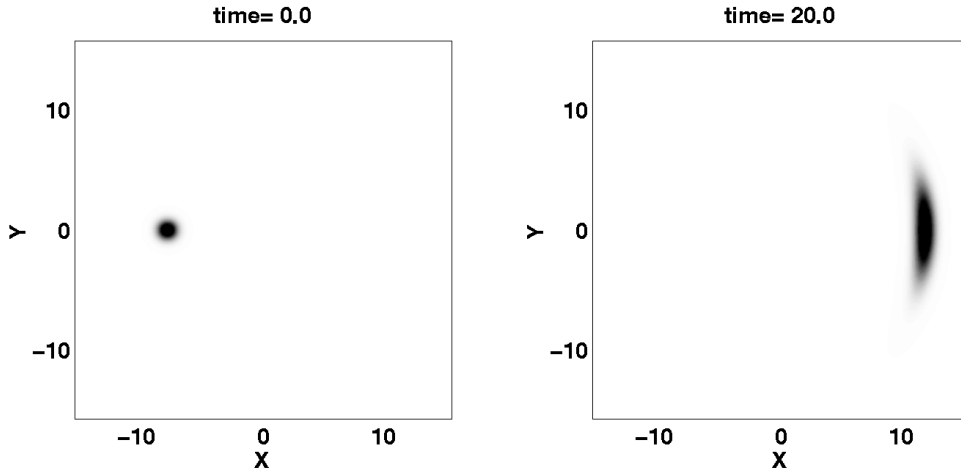


Figure 9: The time evolution of a free photon. The intensity profile of a Gaussian photon does not preserve its shape. The deformation of the profile is fast if the distribution in \mathbf{k} -space has a large variance and is centered close to the origin i.e. has a short wave length.

The initial state in this simulation is a Gaussian (76) and centered close to the origin of \mathbf{k} -space with a large variance. This means that the \mathbf{k} -vectors of the modes with nonzero coefficients are not parallel. The intensity does not preserve its original shape but spreads to a larger area as time increases, which is seen from Fig. 9. The spreading is slower if the Gaussian distribution is centered far from the origin and the variance is small. In that case the \mathbf{k} -vectors of all the modes with nonzero coefficients are almost unidirectional. However the spreading cannot be totally avoided for multimode fields.

7.2.2 A mirror

The atoms can be used to build a mirror for the radiation. The initial setup of the system is shown in Fig. 10. In the left picture there is a photon which propagates to the right. The wave length of the photon is large so we would expect a deformation of

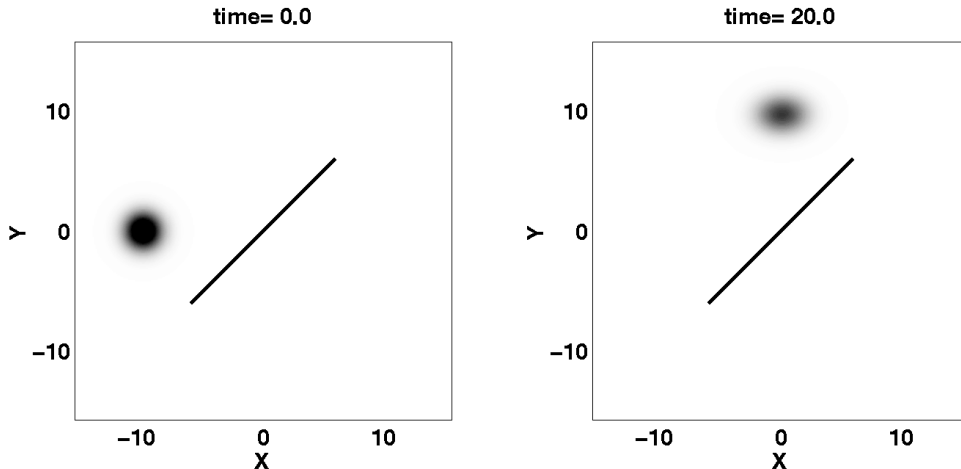


Figure 10: In the center there are several layers of two-level atoms. On the left the photon is propagating towards the atoms. The distance of the atoms in a grid is shorter than the wave length of the photon. The photon is on resonance with the atoms. At $t = 20.0$ the photon has reflected from the atoms so the atoms form a mirror for the photon. The reason for the change of the intensity profile is the same as in Fig. 9.

the intensity profile as in a simulation of a free photon. In the center there is a group of atoms. The atoms are exactly on resonance with the photon and form a multilayer plate. The photon propagates towards the atoms and as can be seen from Fig. 10, right picture, almost all intensity is reflected. The atoms form an almost perfect mirror for the radiation provided that the distances between the atoms are shorter than the wave length of the photon. The intensity profile of the reflected photon is not exactly symmetric. The reason for this is the same as in the simulation of a free photon i.e. the wave length of the photon is short. Figure 12 (left) shows the photon at the mirror. The part which has already been reflected interferes with the incoming part. There is no intensity which would pass the atoms to the right.

7.2.3 A beam splitter

It is also possible to build a beam splitter using two-level atoms. In this simulation we have one layer of atoms in the center. The essential point is that now the frequency of the photon is detuned above the resonance frequency of the atoms. The photon propagates towards the atoms. Part of the radiation is reflected and the rest passes

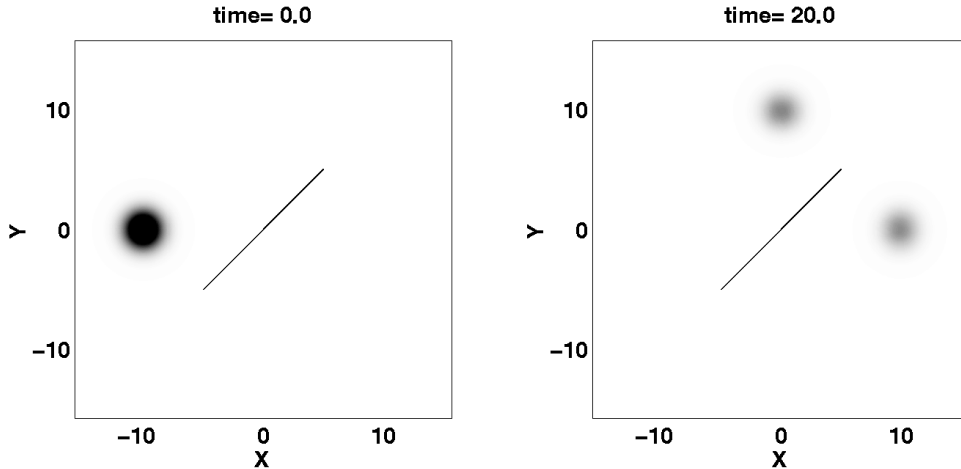


Figure 11: In the center there is one layer of atoms. A photon propagates from the left to the center. The resonance frequency of the photon is detuned above the resonance frequency of the atoms. At $t = 20.0$ half of the intensity has reflected and half has passed the atoms. Thus the atoms form a beam splitter for the incoming radiation.

the atoms. The detuning has been chosen in such a way that we have a 50/50-beam splitter. The photon at the beam splitter is shown in Fig. 12(right). On the left from the beam splitter there is an interference structure as in the mirror simulation. The shorter wave length of the photon is clearly seen from the interference structure. On the right from the beam splitter there is only outgoing radiation and no interference. The shapes of the two parts are more circular than the reflected radiation was in the mirror simulation. This is because the wave length of the photon is shorter here.

We have studied the spectrum of the two outgoing parts using the analyser atom method described in section 5.5. Both spectra were the same and identical to the initial Gaussian spectrum. This is important when we build networks of beam splitters. Exactly the same atomic parameters can be used for additional beam splitters after the two outputs from the first beam splitter.

7.2.4 A parabolic mirror

Mirrors can have arbitrary shapes. In the simulation, Fig. 13, a photon is propagating towards a parabolic mirror. A little circle shows the focus of the parabola. The photon is reflected from the mirror. The familiar interference structure reveals that the wave length is quite long. At $t = 12.8$ the intensity is centered at the focus. The intensity of the photon is here more concentrated than the intensity of the original Gaussian photon. Classically, all intensity goes through the focus and the situation is similar in a quantum mechanical simulation. At later times the photon propagates to the left.

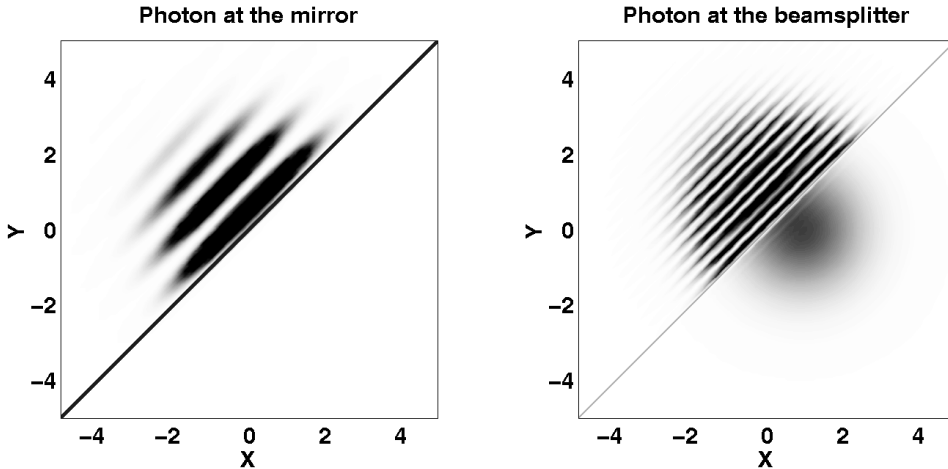


Figure 12: On the left photon is reflecting from the mirror. The incoming and reflected parts interfere. There is no radiation which would pass the atoms. The interference structure reveals the wave length of the photon. On the right a photon is at the beam splitter. Left from the mirror there is an interference structure. The wave length is shorter than in the mirror simulation. Part of the radiation is not reflected but propagates through the atoms.

7.2.5 A mirror box

The next simulation shows interesting interference effects. Three mirrors are arranged to form a box-like structure, Fig. 14. There is no mirror on the left side of the box. Inside the mirrors there is a beam splitter. The photon comes to the box from the left. It is divided into two parts at the beam splitter. The parts reflect from the mirrors back to the beam splitter. Now the two part are united and there is intensity going downwards only. This is because the two parts coming from up and right have different phases and they interfere destructively on the left from the beam splitter. The mirrors reflect the parts back to the beam splitter and the photon is divided again. When the photon comes to the beam splitter for the fourth time it finally escapes from the box. This simulation shows nicely that the intensity at the two outputs of the beam splitter have different phases. We have studied the phase changes more carefully using a Michelson interferometer.

7.2.6 Circular cavities

Using mirror atoms it is possible to build cavities of arbitrary shape. We show a simulation with a circular cavity as an example. The initial state of the field is a superposition of many random Gaussian photons. The radiation is trapped inside the

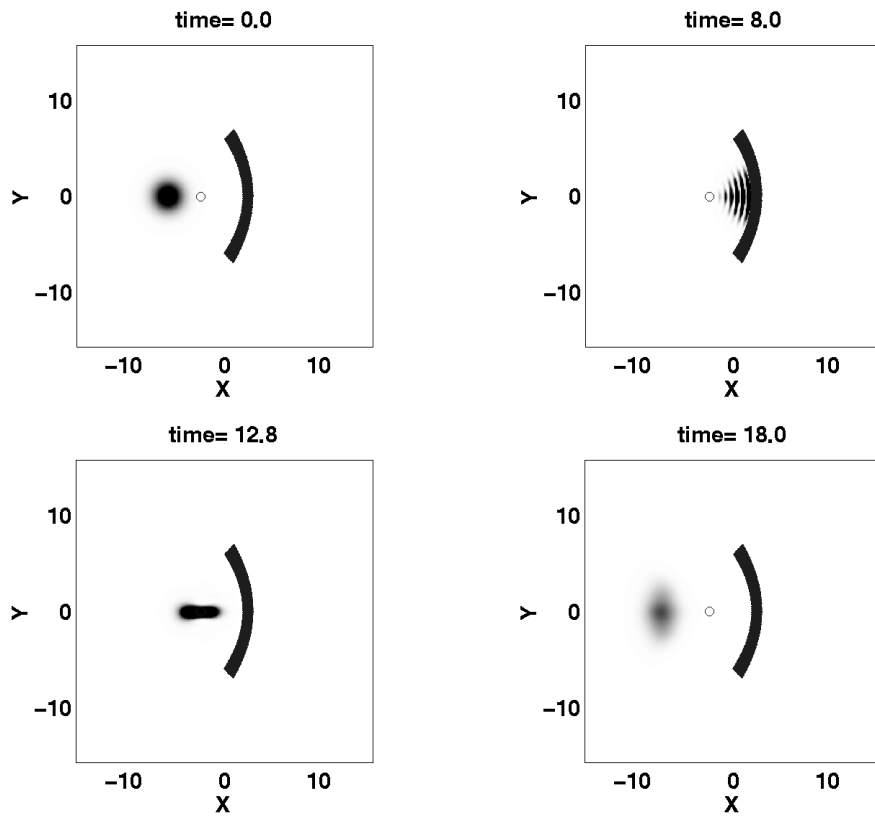


Figure 13: A photon reflects from the parabolic mirror. The little circle shows the focus of the parabola. At $t = 8.0$ the photon reflects from the mirror. At $t = 12.8$ the intensity is centered at the focus. Later the photon spreads and propagates to the left.

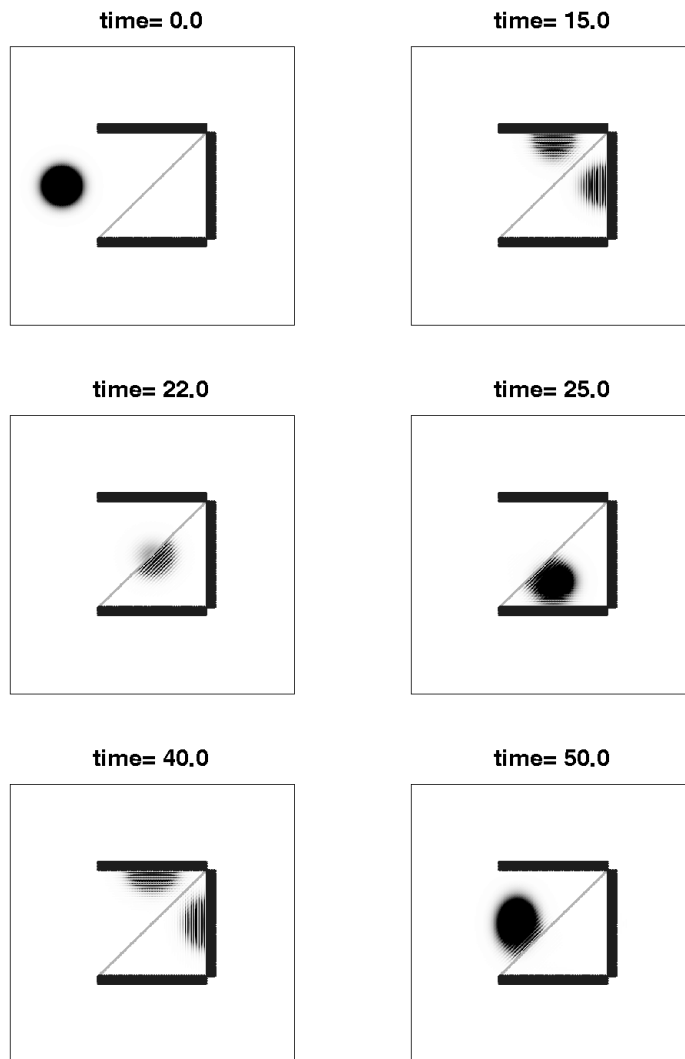


Figure 14: In the center there is a mirror box and a beam splitter. The photon propagates into the box. The beam splitter divides the photon and at $t = 22.0$ unifies it again. The photon reflects from the lower mirror and is divided again. At $t = 50.0$ the photon escapes from the box.

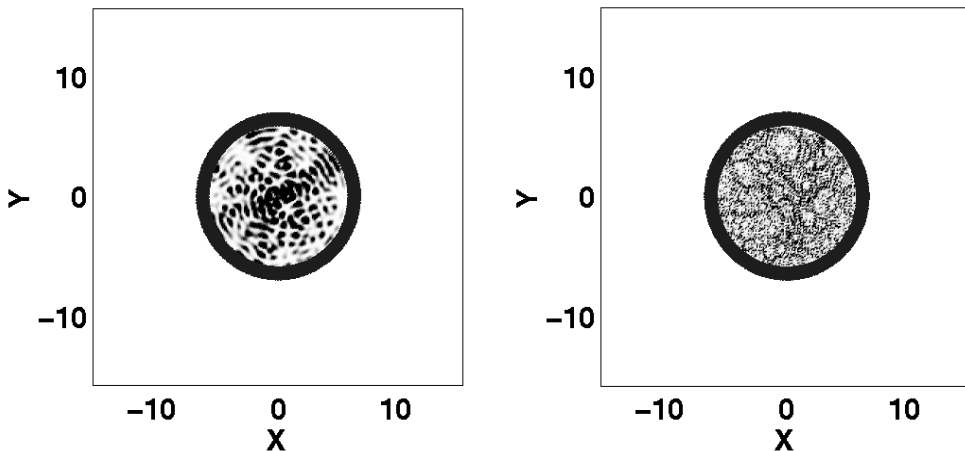


Figure 15: A photon is inside a circular cavity built using two-level atoms. The intensity is trapped inside and the profile remains similar for a long time. On the left the wave length is longer than on the right, which is seen from the interference structure.

cavity. After a time long enough, the radiation is reflected many times and spread to the whole cavity. The typical intensity profile has a 'boiling' structure which has details characterized by the wave length of the photon. Figure 15 shows the typical intensity profile for two different wave lengths. On the left the wave length is large and the bubbles in the intensity are bigger than on the right where the wave length is short.

7.2.7 Decay of an atom in a square cavity

We have studied the decay of a two-level atom inside a square cavity. The cavity is built using two-level atoms. The length of the cavity is $L = 4.0$. The mode functions are

$$g_{n,m} = \sin(k_n x) \sin(k_m y), \quad n, m = 1, 2, \dots \quad (78)$$

where $k_n = n\frac{\pi}{L}$. In \mathbf{k} -space the mode functions are δ -peaks at integer points. The atom is located exactly at the center of the cavity. The resonance frequency is $\omega_0 = \sqrt{3^2 + 1^2}\frac{\pi}{L} = \sqrt{10}\frac{\pi}{L}$, so it is on resonance with the modes with indices ± 3 and ± 1 . The dipole constant of the atom is turned on adiabatically and the maximum value

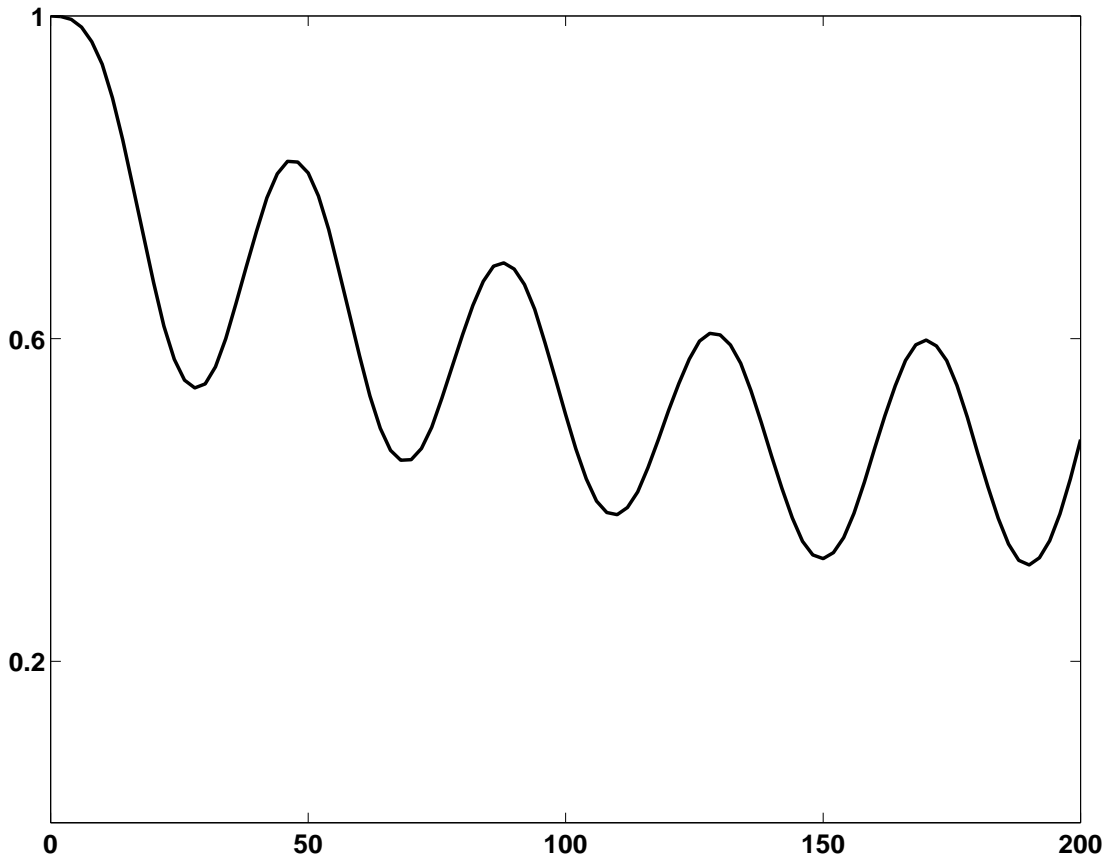


Figure 16: The excitation of the decaying atom in the middle of the square cavity. The atom is on resonance with only a few modes of the cavity. The excitation has an oscillatory behavior.

is very small. Because of the small line width the atom is not on resonance with any other modes. The time evolution of the atomic excitation is shown in Fig. 16. It oscillates and decreases gradually. The intensity profile at $t = 26.0$ is shown in Fig. 17(left). Figure 17(right) shows the excitation of modes at $t = 170$. It is clearly seen that there are four peaks as one would expect based on mode function calculations. Both the intensity and mode excitations oscillate but the profiles remain the same. The problem of an atom interacting with a few modes could be studied also using the Jaynes-Cummings model [51]. It would be interesting to compare the results obtained using two different approaches. It is clear that the simulation with a decaying atom can be used to get information of the mode functions. A topic of recent interest is the form of the mode functions in chaotic semiconductor microcavities [52, 53] which are used to build semiconductor lasers.

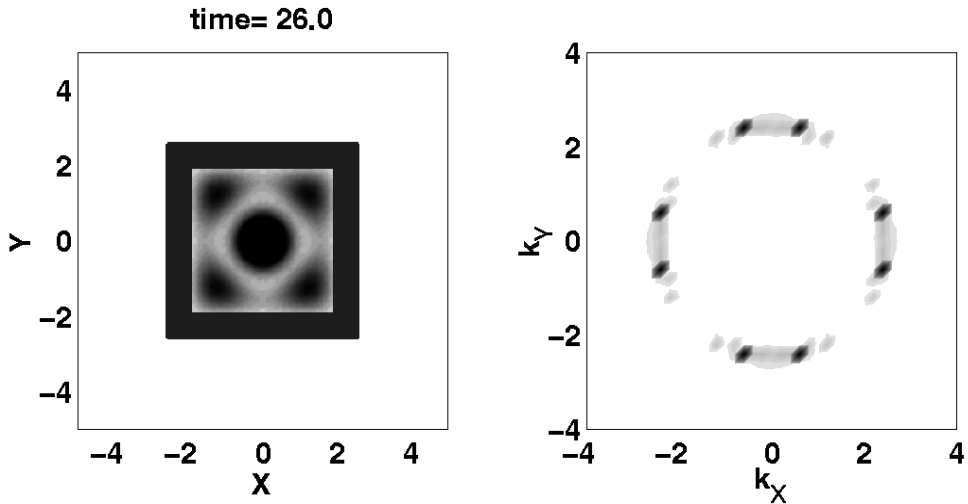


Figure 17: Left: The intensity profile of radiation decayed from the atom inside a square cavity at $t = 26.0$. Right: The excitation spectrum at $t = 170$. There are four peaks at the positions of mode functions. It is clear that the atom interacts only with a few modes.

7.3 Possible future simulations

We have shown several examples of the simulations we have done. It is easy to change the mirror and beam splitter configurations. There are several ways to improve or generalize the current simulations. One extension of the current model would be to use moving atoms. There are cavity QED experiments where excited moving atoms have been guided in between mirrors [54]. When the atom decays, part of the radiation is reflected from the mirrors and absorbed back to the atom. The excitation of the atom should have an oscillating behavior. Using moving atoms it is possible to build moving mirrors and beam splitters. With moving optical components it is possible to study systems which would be very difficult to model using other techniques. It might also be possible to do the simulations in three dimensions. This would allow us to build three-dimensional cavities and follow the time evolution of a photon in three-dimensional optical networks.

One interesting simulation would be to add interaction terms which preserve the excitation number between the atoms. Using interacting atoms, materials with different crystal structures, for example FCC, BCC etc., can be built. Using the method of analyser atoms it is possible to detect the spectrum of the radiation which passes the crystal from different directions. By analyzing the spectra, it is possible to get information on the band structure of the crystal.

8 Conclusion

We have used several different methods to treat the problem of atoms interacting with a quantum mechanical field. In paper I ordinary and cascaded master equations were used. In paper II we used a phenomenological model for the electron dynamics in the electromagnetic trap. In papers III, IV, V and VI the field strength is restricted to one excitation which makes direct integration of the time evolution possible.

We have shown a new method to determine the time-dependent spectrum of radiation. The radiation is directed onto two-level atoms which detect the spectrum. The spectrum can be read from the quantum mechanical state of the atoms. Two time averages and quantum regression theorems are not needed. The method has been used to determine the resonance fluorescence spectrum of a three-level atom (paper I) and the local spectrum of radiation in a one-dimensional cavity (paper IV).

In paper III we have studied the decay of a two-level atom in a one-dimensional cavity. The decay near the cavity mirrors may be faster or slower compared to the free decay depending on the distance from the mirror. The decay in a dielectric material, modelled by two-level atoms, is slower than the free decay.

In our simulations in two dimensions, we have built mirrors and beam splitters using two-level atoms. A mirror can be built using a grid of two-level atoms which are in resonance with the radiation and are close enough to each other. For a beam splitter the atoms have to be off-resonance. It is possible to build complicated optical networks and follow the propagation of radiation through it. We have built plane and parabolic mirrors, interferometers, studied two and one slit experiments etc. Compared to the usual treatment of optical components, in our simulations the whole system, including mirrors and beam splitters, is in a quantum mechanical state. It is also possible to build closed cavities and moving components and study their properties.

Appendix: Numerics

All papers which belong to the thesis are results of extensive numerical simulations. The usual simulation has been the integration of the time evolution of a quantum mechanical system. The system has been described either using state vectors or density matrices. Our choice for the integration routine has usually been the classical fourth order Runge-Kutta algorithm [55]. In some simulations adaptive stepsize routines have been used instead. Most of the simulations have been done using the C++ programming language. In some of the very first programs Fortran 90 was used. We have also done several JAVA applets which can be used to present the simulation results. The program used in the first paper was parallelized using the Message Passing Interface (MPI) [56]. In this section we compare the different languages used, based on our experience. More information about programs etc. can be found from the internet version of the thesis [57].

A.1 Different languages used in the simulations

A.1.1 Fortran

There is no arguing that Fortran has a glorious past. The first versions of Fortran were developed long ago and it was one of the first high level languages, which make it possible to write programs for several different platforms. There are several well defined standardized versions such as Fortran 66, 77, 90, 95... . The version developed in the 70's, Fortran 77, is still used by some conservative programmers. The latest versions are Fortran 90 and 95. The latter has only a few differences compared to Fortran 90. One of the benefits of Fortran is that there has always been a well defined standard, which has been implemented without significant modifications. In scientific calculations multidimensional arrays are used extensively. Fortran 90 has excellent collection of commands which make array manipulations easy. The routines are quite similar to the corresponding MATLAB commands. During the years a lot of different library routines have been developed. Typically these libraries have collections of matrix manipulation functions, Fast Fourier Transforms etc. Because of a long tradition and partly because Fortran is not an object oriented (OO) language, the machine code produced by the compilers is fast and reliable. Also parallelization methods which will be important in future numerics are usually first available to Fortran programmers. One important thing is that Fortran is easier to learn than for example C++.

Perhaps the biggest weakness of Fortran is that it is not an OO language. Even the latest version, Fortran 95, does not support OO features properly. This makes it very

difficult to use Fortran as the only language in bigger projects. There is a new version of Fortran coming out in the beginning of the next millenium [58]. It is planned to have rather big changes to the current version. OO features should be included in a similar way as in C++ and Java. The future of Fortran depends on the success of the forthcoming version of the language.

A.1.2 C and C++

C[59] and C++[60, 61] are very popular languages outside the scientific community. Plain C is a not a very good choice in numerics. Especially the array commands are clumsy compared to Fortran 90 or some C++ class libraries. The other problem is that C is not an OO language.

C++ is the language which has OO features added on top of C. One could argue that it would be better to develop the OO language right from the beginning without using any “base language”. One of the problems is that there has traditionally been several different “dialects” of C++. This makes it difficult to write programs which would compile on several platforms. The standard for C++ [62] was developed a few years ago, but the implementation of the standard by compiler vendors has been slow.

The basic C++ does not have important array commands. It is easy to develop users own array commands because of the OO nature of the language. However, this approach has some weaknesses. First of all, if every user writes personal array commands there will never be a standard. This makes it more difficult to develop interchangeable code. Another weakness which is not so obvious, is that the straightforward implementation techniques tend to give much slower code than the corresponding Fortran routines. There are also other performance problems related to OO features. Some of them have been solved recently using a special template technique in the implementation of the array routines [63]. An array library “Blitz” [64] developed by Todd Veldhuizen, which uses the latest techniques is able to get the performace which is near the corresponding Fortran performance. The popularity of C++ guarantees that there will be good C++ compilers available, even though some people are expecting that JAVA would gradually replace C++ as the leading OO language. Most of the simulations in the present thesis have been done using C++.

A.1.3 Java

Java [65] is a new OO language which has created a lot of excitement during the last few years. The language was originally developed by James Gosling [66] at Sun Microsystems. It has been designed to give programmers better methods to develop

internet applications. The syntax of the language is quite similar to the C++, which makes it easy to learn for most programmers. Many details of C++, which Java programmers think are unnecessary and only make C++ more difficult to learn, have been excluded. One of the main goals of Java is to give users of different computers and operating systems a uniform programming platform. This goal is achieved using the Java Virtual Machine (JVM), which is a low level platform on top of the real hardware. All source code is first compiled to a bytecode, the machine language of the JVM, and it should be possible to run this bytecode on any JVM on any computer. There are already some compilers available, and more will come in the future, which will be able to compile bytecode directly to machine code of different processors. In the future there will probably be special Java chips available, which execute the bytecode directly.

The current situation is that Java is far too slow for any serious scientific calculations, if high performance is needed. The important array commands are missing and it is not easy to implement them properly. There are problems even with the low level features of the language. For example the multiplication of floating point numbers, which should not be a problem for an ordinary programmer, is not properly implemented in JVM. However, the development of Java is now very fast and there is work going on to correct many of the weaknesses mentioned above [67, 68]. I think the best strategy is to follow the development closely and use it to certain specific purposes where performance is not critical. One example of this could be Java applets, which allows simulation results to be shown on web pages. We have used Java for such purpose.

References

- [1] J. D. Jackson, *Classical Electrodynamics*, 2nd. ed. (John Wiley, New York 1975)
- [2] P. A. M. Dirac, Proc. Roy. Soc. (London) **A114**, 243 (1927)
- [3] P. A. M. Dirac, *Principles of Quantum Mechanics*, 4th ed. (Oxford University Press, London 1958)
- [4] L. Mandel and E. Wolf, *Optical Coherence and Quantum Optics* (Cambridge University Press, Cambridge 1995)
- [5] M. O. Scully and M. S. Zubairy, *Quantum Optics* (Cambridge University Press, Cambridge 1997)
- [6] W. H. Louisell, *Quantum Statistical Properties of Radiation* (John Wiley, New York 1973)
- [7] R. Loudon, *The Quantum Theory of Light* (Clarendon Press, Oxford 1973)
- [8] H. J. Carmichael, *An Open Systems Approach to Quantum Optics*, Lecture Notes in Physics, Vol. M18 (Springer, Berlin 1993)
- [9] J. Dalibard, Y. Castin and K. Mølmer, Phys. Rev. Lett. **68**, 580 (1992)
- [10] K. Mølmer, Y. Castin and J. Dalibard, J. Opt. Soc. Am. B **10**, 524 (1993)
- [11] N. Gisin, J. Phys. A **25**, 5677 (1992)
- [12] M. B. Plenio and P. L. Knight, Rev. Mod. Phys. **70**(1), 101 (1998)
- [13] N. Gisin, Phys. Rev. Lett. **52**, 1657 (1984)
- [14] H. J. Carmichael, Phys. Rev. Lett. **70**, 2273 (1993)
- [15] C. W. Gardiner, Phys. Rev. Lett. **70**, 2269 (1993)
- [16] P. Kochan and H. J. Carmichael, Phys. Rev. A **50**, 1700 (1994)
- [17] C. W. Gardiner and A. S. Perkins, Phys. Rev. A **50**, 1722 (1994)
- [18] J. C. Goswami and A. K. Chan, *Fundamentals of Wavelets: Theory, Algorithms and Applications* (Wiley, New York 1999)

- [19] G. Kaiser, *A Friendly Guide to Wavelets* (Birkhäuser, Boston 1994)
- [20] C. K. Chui, *An Introduction to Wavelets* (Academic Press, San Diego 1992)
- [21] A. S. Parkins and D. F. Walls, Phys. Rep. **303**, 1 (1998)
- [22] <http://amo.phy.gasou.edu/bec.html/>
- [23] S. N. Bose, Z. Phys. **26**, 178 (1924)
- [24] A. Einstein, Sitzber. Kgl. Preuss. Akad. Wiss. 1925, 3 (1925)
- [25] M. H. Anderson, J. R. Ensher, M. R. Matthews, C. E. Wieman and E. A. Cornell, Science **269**, 198 (1995)
- [26] K. B. Davis, M.-O. Mewes, M. R. Andrews, N. J. van Druten, D. S. Durfee, D. M. Kurn and W. Ketterle, Phys. Rev. Lett. **75**, 3969 (1995)
- [27] C. C. Bradley, C. A. Sackett and R. G. Hulet, Phys. Rev. Lett. **78**, 985 (1997)
- [28] C. C. Bradley, C. A. Sackett and R. G. Hulet, Phys. Rev. A **55**, R2511 (1997)
- [29] H. G. Dehmelt in *Nobel Lectures, Physics 1981-1990*, edited by G. Ekspong, (World Scientific, Singapore 1993) p. 583
- [30] H. Dehmelt, Am. J. Phys. **58**, 17 (1990)
- [31] L. S. Brown and G. Gabrielse, Rev. Mod. Phys. **58**, 233 (1986)
- [32] F. M. Penning, Physica (Utrecht) **3**, 873 (1936)
- [33] H. Dehmelt, Am. J. Phys. **58**, 17 (1990)
- [34] M. Havukainen and S. Stenholm, Phys. Rev. A **60**, 621 (1999)
- [35] J. D. Cresser, Phys. Rep. **94**, 47 (1983)
- [36] M. Lax, Phys. Rev. **129**, 2342 (1963)
- [37] L. Onsager, Phys. Rev. **37**, 405 (1931)
- [38] N. Gisin, J. Mod. Opt. **40**, 2313 (1993)
- [39] T. Felbinger and M. Wilkens, J. Mod. Opt. **46**, 1401 (1999)

- [40] C. H. Page, J. Appl. Phys. **23**, 103 (1952)
- [41] D. G. Lampard, J. Appl. Phys. **25**, 803 (1954)
- [42] R. A. Silverman, Proc I.R.E. (Trans. Inf. Th) **3**, 182 (1957)
- [43] J. H. Eberly and K. Wódkiewicz, J. Opt. Soc. Am. **67**, 1252 (1977)
- [44] J. H. Eberly, C. V. Kunasz and K. Wódkiewicz, J. Phys. B **13**, 217 (1980)
- [45] M. Havukainen and S. Stenholm, J. Mod. Opt. **45**, 1699 (1998)
- [46] V. Bužek, Czech. J. Phys. B **39**, 345 (1989)
- [47] V. Bužek and M. G. Kim, J. Korean Phys. Soc. **30**, 413 (1997)
- [48] V. Bužek, G. Drobný, M. G. Kim, M. Havukainen and P. L. Knight, Phys. Rev. A **60**, 582 (1999)
- [49] G. W. Ford and R. F. O'Connell, Phys. Rev. Lett. **77**, 798 (1996)
- [50] M. Havukainen, G. Drobný, S. Stenholm and V. Bužek, J. Mod. Opt. **46**, 1343 (1999)
- [51] E. T. Jaynes and F. W. Cummings, Proc. IEEE **51**, 89 (1963)
- [52] J. U. Nöckel and A. D. Stone, Nature **385**, 45 (1997)
- [53] C. G. Gmachl, F. Capasso, E. E. Narimanov, J. U. Nöckel, A. D. Stone, J. Faist, D. L. Sivco and A. Y. Cho, Science **280**, 1556 (1998)
- [54] H. J. Kimble in *Cavity Quantum Electrodynamics*, edited by P. R. Berman, (Academic Press, Boston 1994) p. 203
- [55] W. H. Press, S. A. Teukolsky, W. T. Vetterling and B. P. Flannery, *Numerical Recipes in C*, 2nd ed., (Cambridge University Press, Cambridge 1995)
- [56] <http://www.mpi-forum.org/>
- [57] <http://www.hip.fi/~quantum/theses/havukainen/>
- [58] <http://www.etc.ox.ac.uk/SC22WG5/index.html>

- [59] B. W. Kernighan and D. M. Ritchie, *The C programming language*, 2nd ed., (Prentice Hall, 1988)
- [60] S. B. Lippman and J. L. Lajoie, *C++ primer*, 3rd ed., (Addison Wesley, Reading 1998)
- [61] B. Stroustrup, *The C++ programming language*, 3rd ed., (Addison Wesley, Reading 1997)
- [62] <http://anubis.dkuug.dk/JTC1/SC22/> → C++
- [63] T. Veldhuizen, Dr. Dobb's J. (November 1997) 34; T. Veldhuizen, Dr. Dobb's J. (August 1996) 38; T. Veldhuizen, C++ report, **7**(5), 26 (1995); T. Veldhuizen, C++ report, **7**(4), 36 (1995); N. C. Myers, **7**(5), (1995)
- [64] <http://oonumerics.org/blitz/index.html>
- [65] <http://java.sun.com/>
- [66] <http://java.sun.com/people/jag/>
- [67] <http://www.javagrande.org/>
- [68] <http://math.nist.gov/javanumerics/>